GEOLOGICAL SURVEY OF CANADA
COMMISSION GÉOLOGIQUE DU CANADA

PAPER 80-28

APPLICATIONS OF THERMODYNAMICS IN THE STUDY OF MINERAL DEPOSITS

E. FROESE

Canada

1981

GEOLOGICAL SURVEY
PAPER 80-28

APPLICATIONS OF THERMODYNAMICS IN THE STUDY OF MINERAL DEPOSITS

E. FROESE

1981

Available in Canada through

authorized bookstore agents
and other bookstores

or by mail from

Canadian Government Publishing Centre
Supply and Services Canada
Hull, Québec, Canada K1A 0S9

and from

Geological Survey of Canada
601 Booth Street
Ottawa, Canada K1A 0E8

A deposit copy of this publication is also available
for reference in public libraries across Canada

Cat. No. M44-80/28E Canada: $4.00
ISBN 0-660-10816-X Other countries: $4.80

Price subject to change without notice

Critial Reader

K.L. Currie
J.M. Duke

Manuscript submitted: 1980 - 05 - 05
Approved for publication: 1980 - 07 - 31

CONTENTS

Figures

APPLICATIONS OF THERMODYNAMICS IN THE STUDY OF MINERAL DEPOSITS

Abstract

This paper summarizes the principles of thermodynamics required for an understanding of reaction equilibria in aqueous solutions and outlines the construction of activity diagrams. Making use of the concept of electron activity, the electron is treated as an aqueous species. Mineral stabilities in several types of mineral deposits are portrayed by means of log f_{O_2}-pH diagrams. The metamorphism of sulphide-bearing rocks is discussed in terms of sulphide-oxide-silicate reactions.

Résumé

Cette étude résume les principes de la thermodynamique qui doivent être appliqués pour comprendre l'équilibre des réactions en solutions aqueuses, et elle décrit la structure des diagrammes d'activité. Au moyen de la notion d'activité de l'électron, l'électron est traîté comme des espèces aqueuses. La stabilité des minéraux dans plusieurs types de gîtes est calculée en fonction de log f_{O_2}- pH. Le métamorphisme des roches contenant du sulfure est discuté en termes de réactions de sulfure-oxyde-silicate.

INTRODUCTION AND ACKNOWLEDGMENTS

This paper, a companion volume to Geological Survey of Canada Paper 75-43 (Froese, 1976), deals with the application of thermodynamics to a few examples of interest in the study of mineral deposits. Selected topics are discussed in terms of reaction equilibria with an attendant emphasis on the equilibrium constant. The prominence of reactions in aqueous solutions in the examples here considered requires an extension of the theoretical background given in Paper 75-43. In approach and in notation, the treatment keeps very close to the presentation of thermodynamics by Denbigh (1971) and familiarity with this book will be assumed.

This paper is based on a series of lectures given at the University of Göttingen in October 1979 at the invitation of the Sonderforschungsbereich Göttingen of the Deutsche Forschungsgemeinschaft. I am very grateful for the invitation and for financial support which made this visit possible. The original lecture notes have been revised in response to comments from the audience and other interested persons. In particular, I have benefitted from discussions with T.M. Gordon, K.L. Currie and M.J. Duke. A thesis submitted by P.A. Goetz to Carleton University prompted me to become better acquainted with the topic of sulphide solubility. In the development of the activity concept, I have been considerably influenced by G. Tunell, through discussions and access to his unpublished Notes on Chemical Thermodynamics, and by the late L.S. Darken through his lengthy and remarkably patient letters. I am also pleased to acknowledge H. Winkler's encouragement, over a number of years, to pursue my interests in thermodynamics. The diagrams in this paper have been drafted by J. MacManus.

In this publication, the scope of the original lectures has been retained. Consequently, only a few selected topics are treated, with a modest goal in mind: an introduction to the construction of geologically useful activity diagrams based on thermochemical data. The most regrettable omission is the lack of discussion of the derivation, consistency, and uncertainty of thermochemical data.

THERMODYNAMIC BASIS

Reaction Equilibrium

In thermodynamic analysis, a system refers to a portion of matter, or to a given volume, which is separated from its surroundings. The thermodynamic state of a system is characterized by macroscopic properties or state variables. If the state variables persist unchanged over a period of time, the system is considered to be in equilibrium. At equilibrium, state variables are interrelated. Thermodynamics accepts pressure (P) and volume (V) as state variables known from mechanics and deduces three new state variables: temperature (T), internal energy (U), and entropy (S). In this paper, the following combined statement of the first and second laws will be accepted

$$\left(dU_{sy} + PdV_{sy} - TdS_{sy}\right) \leqq 0$$

This equation describes the relations among the state variables within a closed system. The subscript "sy" emphasizes that the extensive properties U,V, and S refer to the total amount of matter contained in the system. The equality refers to reversible changes and to those changes involving irreversible transfer of heat and work between the system and the surroundings. The inequality refers to irreversible chemical changes (Everdell, 1965). If constant P and T can be imposed on the system

$$d\left(U_{sy} + PV_{sy} - TS_{sy}\right) \leqq 0$$

The combination of variables (U + PV − TS) is known as the Gibbs free energy (G). Thus

$$dG_{sy} \leqq 0$$

Chemical changes lead to a change in the mole numbers of chemical species. At constant P and T, the Gibbs free energy of a system is a function of the mole numbers and may be differentiated to give

$$dG_{sy} = \sum \left(\frac{\partial G_{sy}}{\partial n_i} \right)_{n_j} dn_i$$

where n_i refers to a particular chemical species and n_j to all other species.

This is a general relationship valid for closed as well as open systems. If it is applied to a closed system, however, not all changes of mole numbers can be independent. A chemical reaction represents a change within a closed system and, because of the stoichiometric restriction of the reaction equation, there is only one independent change in the number of moles. In the generalized reaction equation

$$\sum \nu_i M_i = 0$$

M represents the chemical formula of a species and ν the stoichiometric coefficient, taken as positive for products and negative for reactants. Following De Donder (1920) and Schottky et al. (1929), the extent of reaction (ξ) is defined by

$$d\xi = \frac{dn_i}{\nu_i}$$

The extent of reaction (ξ) can vary from 0 to 1.

By defining the partial molar free energy of a species as

$$\bar{G}_i = \left(\frac{\partial G_{sy}}{\partial n_i} \right)_{P,T,n_j}$$

the following relationship is obtained

$$\left(\frac{\partial G_{sy}}{\partial \xi} \right)_{P,T} = \sum \nu_i \bar{G}_i$$

Plotting G_{sy} against ξ, it is seen that $\Sigma \nu_i \bar{G}_i$ represents the difference in the intercepts, at $\xi = 0$ and at $\xi = 1$, of a tangent to the free energy curve (Fig. 1). If this curve has a minimum, the reaction will stop at the corresponding value of ξ; if there is no minimum, the reaction will proceed to completion.

At the minimum

$$\left(\frac{\partial G_{sy}}{\partial \xi} \right)_{P,T} = \sum \nu_i \bar{G}_i = 0$$

and the reaction is reversible, i.e. there is no tendency for spontaneous change because the system has reached its lowest energy state. The expression $\nu_i \bar{G}_i$ has commonly been designated as ΔG

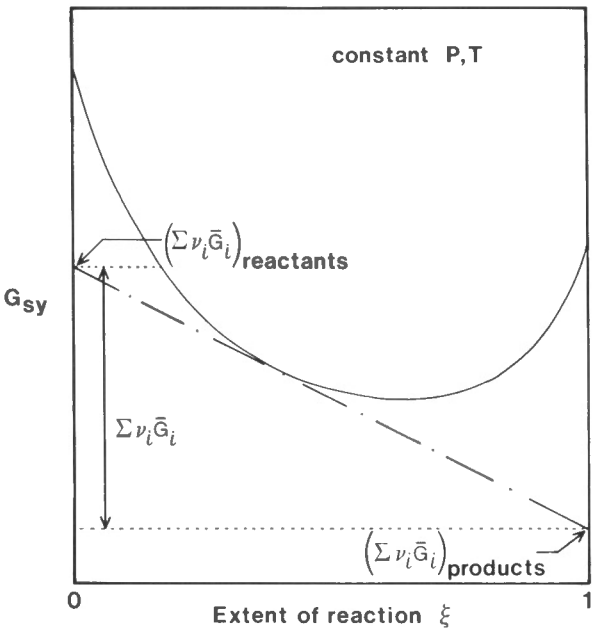

Figure 1

The variation of the Gibbs free energy of a system (G_{sy}) with the extent of reaction (ξ).

and referred to as the Gibbs free energy change of a reaction. Spencer (1974) pointed out that the symbol Δ should be reserved for differences in G_{sy} between two points on the free energy curve. However, in view of the long-standing practice, the conventional use of $\Delta G = \nu_i \bar{G}_i$ is here accepted.

At any particular value of ξ, the state variables of the system are defined. For this reason, the system is in a state of equilibrium. But this state can only be realized if the system can be restrained from further reaction at a particular value of ξ. Accordingly, Schottky et al. (1929) referred to this state as "arrested" equilibrium. If the system is allowed to react until $\Sigma \nu_i \bar{G}_i = 0$, it is in a state of stable equilibrium, commonly called reaction equilibrium, which is true only for a particular value of ξ.

In order to evaluate the expression $\Sigma \nu_i \bar{G}_i$, the attention is turned from the properties of the system as a whole, to the molar properties of the species. The species may be present either as pure phases or as components in phases of variable compositions. And here a hurdle of conceptual and practical difficulties is encountered. Although the state variables of a homogeneous substance (e.g. one mole of a solution of fixed composition) are well defined, the molar property of a solution is generally not of prime interest. Chemical reactions involve individual components of solutions. Some components in a solution may not take part in the reaction; the boundary of the closed system represented by the reaction must be placed through the solution so as to include some components but not necessarily all components. It is required to know the property associated with one mole of a substance as it exists in solution. This concept is an abstraction, because in physical reality components do not exist as separate entities and do not possess individual shares of the total property. However, it is possible to "divide" the total property among the components by means of the mathematical device of partial differentiation. The free energy of a phase (like the free energy of any system) is a function of the mole numbers in the phase and may be differentiated to give the partial molar free energy of a species

$$\bar{G}_i = \left(\frac{\partial G_{phase}}{\partial n_i} \right)_{P,T,n_j}.$$

The term "partial" is inherited from the mathematical process; it must be remembered that the property refers to one mole of a component in solution, not to part of a mole.

Thus the molar Gibbs free energy of a substance in solution is not only determined by P and T but also by its concentration and usually also by the concentration of other components. The variation of $\bar{G}$ with these parameters must be considered next.

Definition of Standard States and Energy Datum

In determining the sign of $\Sigma \nu_i \bar{G}_i$ it is necessary to compare $\Sigma \nu_i \bar{G}_i$ of products with $\Sigma \nu_i \bar{G}_i$ of reactants. This can be done by measuring the free energy content of both sides of the reaction equation with respect to the same datum. Since all substances are assembled from elements, these have been assigned zero energy content at any temperature at a specified condition known as the standard state. For solids and liquids, this is the pure element at one atmosphere* and for gases it is the perfect gas at one atmosphere.

The partial molar Gibbs free energy of a substance with respect to the elements may be divided into three energy changes (Fig. 2):

1. The energy change in preparing one mole of the substance in its standard state from the elements in their standard states. This is known as the standard Gibbs free energy of formation ΔG_f°. This energy change is defined only if the standard state is specified.

   Solids: pure substance at one atmosphere

   Gases: perfect gas at one atmosphere

   Liquids: either a) the pure substance at one atmosphere
   or b) the hypothetical one-molal solution at one atmosphere.

   The molar Gibbs free energy of a substance in its standard state is indicated by G°.

2. The energy change in taking the substance from its standard state to a different pressure without changing the composition. For solids and gases this is given by the difference (G^*-G°) where G^* is the molar Gibbs free energy at some specified pressure P^*. For liquids, the energy change is given either by (G^*-G°) or by $(\bar{G}^\square-G^\circ)$ where $\bar{G}^\square$ is the partial molar Gibbs free energy of the substance in the hypothetical one-molal solution at some specified pressure.

3. The energy change in taking a substance, at constant P^*, from its pure state or from a one-molal solution to a solution of a certain composition. This change is given by $(\bar{G}-G^*)$ and $(\bar{G}-\bar{G}^\square)$, respectively.

Thus the partial molar Gibbs free energy of a substance with respect to the elements in their standard states is

$$\bar{G} = \Delta G_f^\circ + (G^*-G^\circ) + (\bar{G}-G^*)$$

or

$$\bar{G} = \Delta G_f^\circ + (G^\square-G^\circ) + (\bar{G}-G^\square)$$

* 1 atmosphere = 1.01325 bars = 101.325 kPa

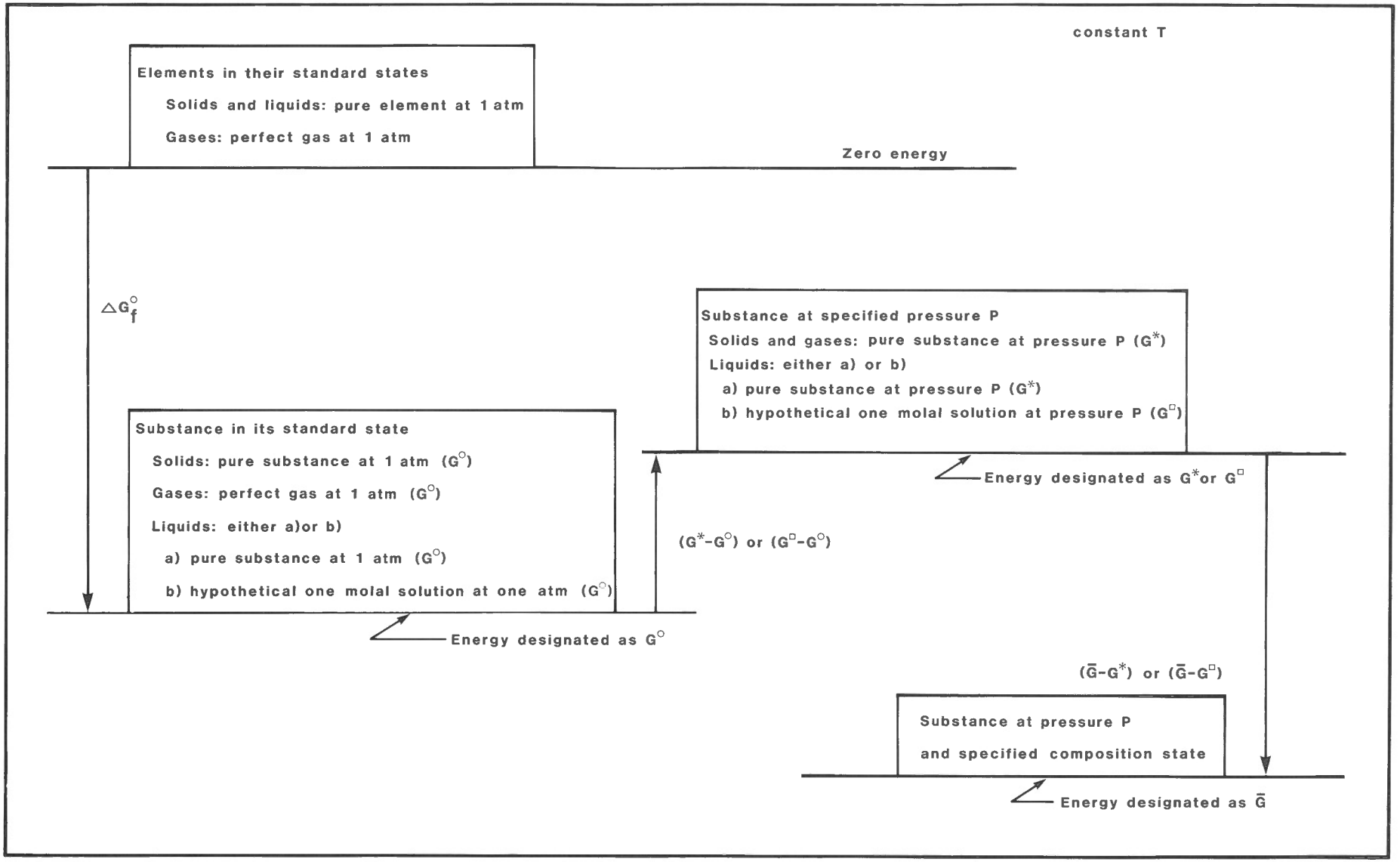

Figure 2. *The partial molar Gibbs free energy of a substance with respect to the elements in their standard states.*

Before evaluating the Gibbs free energy change of a reaction, it is necessary to substitute measureable quantities for the last two energy differences of each substance. Consequently, the variation of $\bar{G}$ with composition X and pressure P must be considered.

The Variation of $\bar{G}$ with Composition

The greatest obstacle in applied thermodynamics concerns the evaluation of the energy differences $(\bar{G}-G^*)$ and $(\bar{G}-G^\square)$ because thermodynamics does not provide a simple relationship for the variation of $\bar{G}$ with composition. Attempts to overcome this difficulty produced the activity concept which uses some limiting conditions imposed by the Gibbs-Duhem equation together with nonthermodynamic observations.

The partial molar Gibbs free energies of components in a solution cannot be varied independently. At constant pressure and temperature, their interdependence is given by the Gibbs-Duhem equation (for a derivation see Denbigh, 1971). For a binary solution at constant pressure and temperature, the Gibbs-Duhem equation is

$$n_1 d\bar{G}_1 + n_2 d\bar{G}_2 = 0$$

Dividing by $(n_1 + n_2)$ and considering specifically the variation with dX_2 at constant pressure and temperature

$$X_1 \left(\frac{\partial \bar{G}_1}{\partial X_2}\right)_{P,T} + X_2 \left(\frac{\partial \bar{G}_2}{\partial X_2}\right)_{P,T} = 0$$

or somewhat rearranged and dropping the subscripts

$$\left(\frac{\partial \bar{G}_1}{\partial X_2}\right) \Big/ \left(\frac{\partial \bar{G}_2}{\partial X_2}\right) = -\frac{X_2}{X_1}$$

where X is the mole fraction.

This equation indicates two possible types of behaviour at infinite dilution (Fig. 3). As $X_2 \to 0$,

either (case 1)	or (case 2)
$\left(\frac{\partial \bar{G}_1}{\partial X_2}\right)$ remains finite	$\left(\frac{\partial \bar{G}_1}{\partial X_2}\right) \to 0$
and	and
$\left(\frac{\partial \bar{G}_2}{\partial X_2}\right) \to -\infty$	$\left(\frac{\partial \bar{G}_2}{\partial X_2}\right)$ remains finite

Case 1 is observed if the mole fraction of component 2 cannot have negative values; case 2 is observed if the mole fraction of component 2 can have negative values (Gibbs, 1876). Considering a solution of two substances A and B, case 1 corresponds to a choice of components such that component 1 is pure A. Case 2 corresponds to choosing an intermediate composition between A and B

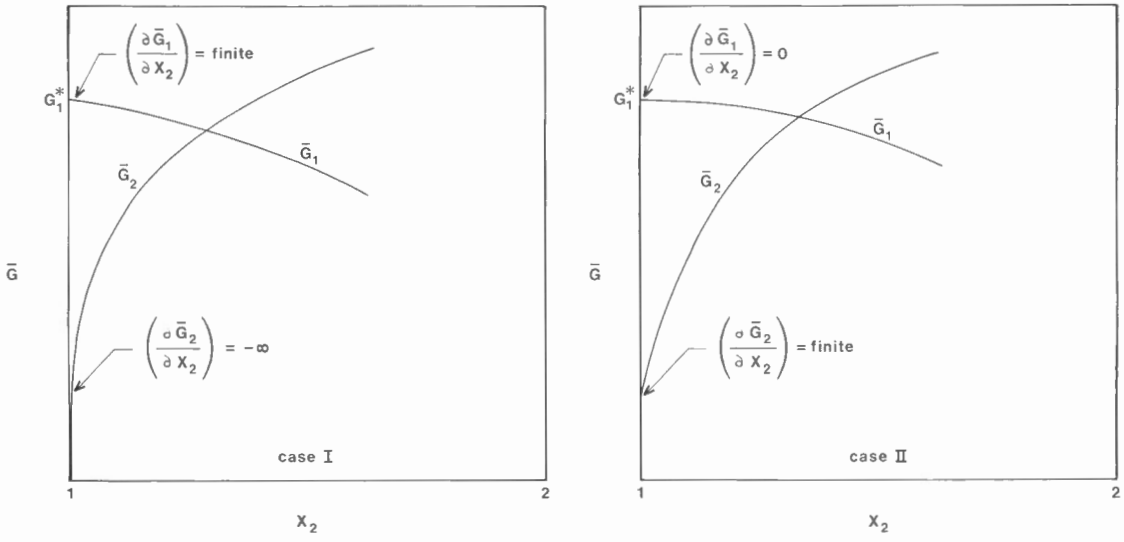

Figure 3. *The variation of the partial molar Gibbs free energies of the components of a binary solution with composition.*

as component 1; in such a case, the mole fraction of component 2 will have a negative value if the composition of the solution lies between A and the composition of component 1. The first case is commonly illustrated in textbooks (e.g. Lewis and Randall, 1961, p. 212).

The Gibbs-Duhem equation for a binary solution is

$$-X_1 \left(\frac{\partial G_1}{\partial X_2}\right)_{P,T} = X_2 \left(\frac{\partial G_2}{\partial X_2}\right)_{P,T}$$

and, since $dX_2 = -dX_1$, it may be written in the form

$$\left(\frac{\partial \bar{G}_1}{\partial \ln X_1}\right)_{P,T} = \left(\frac{\partial \bar{G}_2}{\partial \ln X_2}\right)_{P,T}$$

Considering case 1, if $X_2 \to 0$, $(\partial \bar{G}_1/\partial X_2)$ remains finite. For this reason, $(\partial \bar{G}_1/\partial \ln X_1)$ and $(\partial \bar{G}_2/\partial \ln X_2)$ also remain finite. It is also observed that this slope is, in general, a multiple of RT and that one particular choice of the formula weight of component 2 will make the slope equal to RT (Adams, 1936). It is convenient, therefore, to define an ideal solution by the relation

$$\left(\frac{\partial \bar{G}}{\partial \ln X}\right)_{P,T} = RT$$

Thus limiting ideal behaviour demands two prerequisites:

1. The mole fraction of the component which approaches zero cannot have negative values.
2. One particular folmula weight must be chosen for the component the mole fraction of which approaches zero, e.g. $MgSiO_3$ rather than $Mg_2Si_2O_6$.

If these conditions are fulfilled, as $X_2 \to 0$ and $X_1 \to 1$, both components become ideal; component 2 follows Henry's Law and component 1 follows Raoult's Law.

So far no restrictions have been made on the nature of component 1. There is, however, considerable advantage in choosing it in such a way that Henry's Law is approached at infinite dilution. Many solution models require the boundary condition that Raoult's Law and Henry's Law are approached at both ends of the composition scale. The following conventions of expressing the behaviour of $\bar{G}$ with composition imply such boundary conditions. Before proceeding, there looms the unfortunate task of considering molality as a measure of concentration. The molality is defined as the number of moles of solute per 1000 g of solvent. Thus the molality and mole fraction are related by

$$X = \left(\frac{m}{m+n}\right)$$

where n refers to the number of moles of solvent. This is a constant, in the case of water equal to 55.55. Taking the logarithm and differentiating with respect to ln m

$$\ln X = \ln m - \ln (m+n)$$

$$\left(\frac{d \ln X}{d \ln m}\right) = 1 - \left(\frac{d \ln (m+n)}{d \ln m}\right)$$

$$= 1 - \left(\frac{d \ln (m+n)}{d (m+n)}\right) \left(\frac{d (m+n)}{dm}\right) \left(\frac{d m}{d \ln m}\right)$$

$$= 1 - \left(\frac{1}{m+n}\right) (1) \quad (m)$$

$$= 1 - X$$

As $X \to 0$, $d \ln m \to d \ln X$ and the expression

$$\left(\frac{\partial \bar{G}}{\partial \ln m}\right)_{P,T} = RT$$

will plot as a curved line on a diagram of $\bar{G}$ vs. ln X but as $X \to 0$, the slope $\to$ RT (Fig. 4). This relation defines the hypothetical solution. There now exists a framework for defining activity coefficients and activities according to three conventions, using either Raoult's Law, Henry's Law, or the hypothetical solution as the norm and expressing the deviation from it by a RT ln γ term, where γ is the activity coefficient:

Convention I

$$\bar{G} - G^* = RT \ln X + RT \ln \gamma_{rl} = RT \ln a_{rl}$$

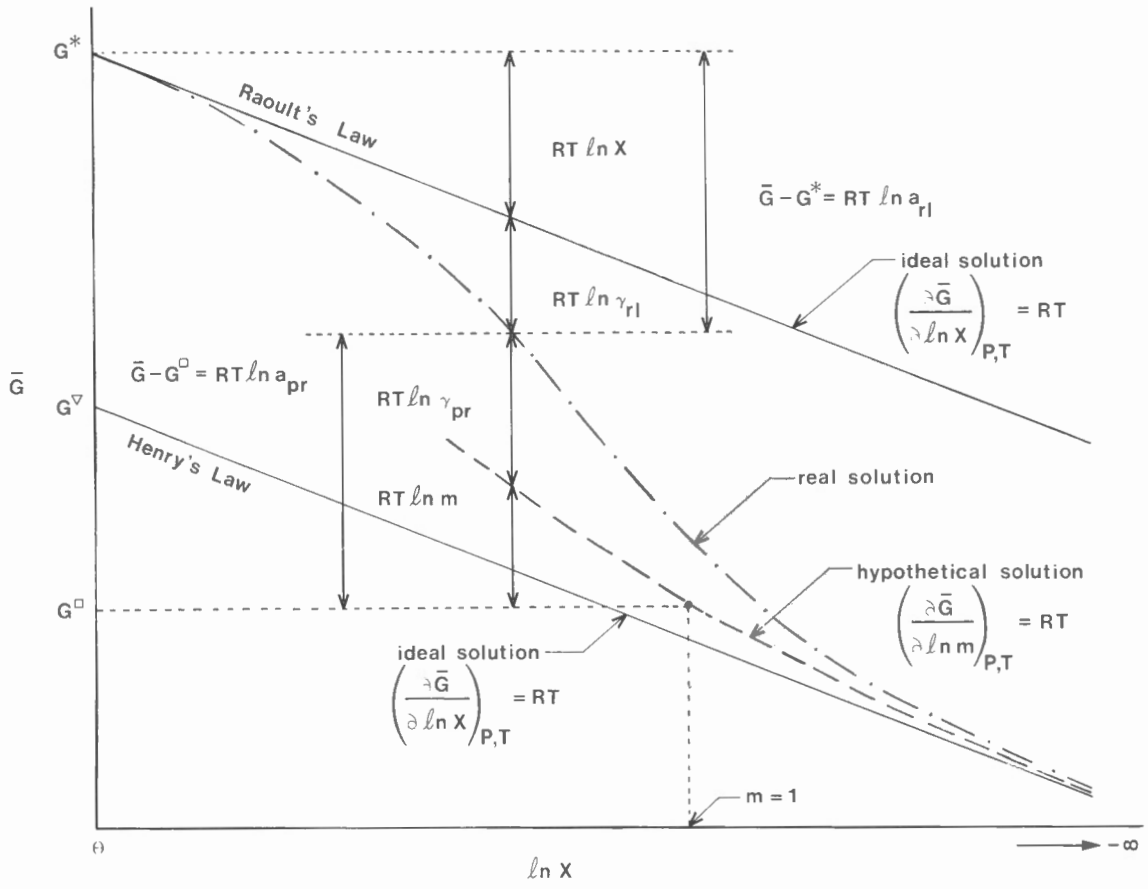

Figure 4. *Definitions of activity and activity coefficient.*

Convention II

$$\bar{G} - G^{\triangledown} = RT \ln X + RT \ln \gamma_{hl} = RT \ln a_{hl}$$

(Note that Denbigh (1971) uses μ^* (equivalent to G^*) instead of $G^{\triangledown}$, but μ^* in Convention II is not the same as in Convention I)

Convention III

$$\bar{G} - \bar{G}^{\square} = RT \ln m + RT \ln \gamma_{pr} = RT \ln a_{pr}$$

The subscripts "rl", "hl", and "pr" stand for Raoult's Law, Henry's Law, and practical. Convention I is used for non-electrolyte solutions and Convention III for aqueous solutions. Convention II is rarely used. The subscripts are commonly dropped and the type of activity and activity coefficient must be gleaned from the context.

The Variation of $\bar{G}$ with Pressure

Instead of evaluating the effect of pressure on $\bar{G}$ for each particular composition it is convenient to look only at the variation of G^* and $G^{\square}$ (i.e. the unit-activity states) with pressure. For this purpose, the following generally valid relationship is integrated

$$\left(\frac{\partial G}{\partial P}\right)_T = V$$

Thus for solids

$$G^* - G^\circ = \int_1^P V \, dP$$

where V is the molar volume of the pure substance.

For liquids either the same relationship may be used or

$$G^{\square}-G^{\circ} = \int_{1}^{P} \bar{V}^{\infty} dP$$

where $\bar{V}^{\infty}$ is the partial molar volume at infinite dilution (a species conforming to the hypothetical solution model has, at all compositions, a partial molar volume equal to that at infinite dilution).

For gases it is customary to integrate the formula for a perfect gas, thus obtaining

$$G^{*}-G^{\circ} = RT \ln P/P^{\circ}$$

where P° is one atmosphere and commonly omitted in the equation.

The molar Gibbs free energy of a real gas is given by

$$G^{*}-G^{\circ} = RT \ln P/P^{\circ} + RT \ln \varphi$$

where $RT \ln \varphi$ is a deviation term given by

$$RT \ln \varphi = \int_{P=0}^{P} (V^{real}-V^{perf}) dP$$

and φ is the fugacity coefficient. Defining fugacity f as equal to $P\varphi$ (Tunell, 1931), it follows from

$$G^{*}-G^{\circ} = RT \ln \left(\frac{P\varphi}{P^{\circ}}\right)$$

that a real gas at G° has a fugacity, designated as f°, equal to P°. Thus

$$G^{*}-G^{\circ} = RT \ln (f/f^{\circ})$$

where f° is equal to one atmosphere and is usually omitted. Commonly this fugacity ratio is used in calculations; it may be regarded as being defined in terms of an energy difference.

The Variation of $\bar{G}$ with Pressure and Composition for Gases

For gases it is common practice to combine the variation of $\bar{G}$ with pressure and composition as follows

$$\begin{aligned} G^{*}-G^{\circ} &= RT \ln (P/P^{\circ}) + RT \ln \varphi \\ \bar{G}-G^{*} &= RT \ln X + RT \ln \gamma \\ \hline \bar{G}-G^{\circ} &= RT \ln \left(\frac{P\varphi X\gamma}{P^{\circ}}\right) \end{aligned}$$

The fugacity of a species in a gaseous solution is defined by $f = P\varphi X\gamma$. Consequently, the gas species at G° has a fugacity, designated as f°, equal to P° and

$$G - G^{\circ} = RT \ln (f/f^{\circ})$$

The fugacity ratio, defined by an energy difference is used in calculations but f°, equal to one atmosphere, is commonly omitted. For a perfect gaseous species ($\varphi=1$) in an ideal solution ($\gamma=1$) the fugacity is equal to the partial pressure PX.

The Equilibrium Constant

The Gibbs free energy change of a chemical reaction is given by

$$\Delta G = \sum \nu_i \bar{G}_i$$

where ν_i is the stoichiometric coefficient and $\bar{G}_i$ the partial molar Gibbs free energy of each substance taking part in the reaction. In order to evaluate ΔG, it is necessary to have measurable values of $\bar{G}$. The variation of $\bar{G}$ of a substance with pressure and composition is summarized in Table 1. For each substance, it is possible to express $\bar{G}$ by the sum of ΔG_f° and energy increments due to the variation of pressure and composition from the standard conditions. Making such substitution for $\bar{G}$

$$\Delta G = \Delta G^{\circ} + \int_{P=1}^{P} \Delta V dP + \int_{P=1}^{P} \Delta \bar{V}^{\infty} dP + RT \ln Q$$

In this formula, ΔG° is the standard Gibbs free energy change of the reaction, ΔV refers to the volume change due to those substances for which the standard state is X = 1 and $\Delta \bar{V}^{\infty}$ to the volume change due to those substances for which the standard state is m = 1. The quotient Q consists of fugacities and activities each raised to a power equal to the stoichiometric coefficient.

Table 1. The variation of $\bar{G}$ with pressure and composition

	Thermodynamic relation	Model substance	Integrated equation: Model substance	Integrated equation: Real substance	$(\bar{G} - G^\circ)$ of a substance at specified P and X
Gases Standard state: perfect gas at 1 atm	$\left(\frac{\partial G}{\partial P}\right)_T = V$	$PV = RT$	$G^* - G^\circ = RT \ell n \frac{P}{P^\circ}$	$G^* - G^\circ = RT \ell n \left(\frac{P\varphi}{P^\circ}\right)$	$\bar{G} - G^\circ = RT \ell n \frac{f}{f^\circ}$
		$\left(\frac{\partial \bar{G}}{\partial \ell n X}\right)_{P,T} = RT$	$\bar{G} - G^* = RT \ell n X$	$\bar{G} - G^* = RT \ell n (X\gamma)$	
Solids and liquids Standard state: pure substance at 1 atm	$\left(\frac{\partial G}{\partial V}\right)_T = V$			$G^* - G^\circ = \int_1^P V dP$	$\bar{G} - G^\circ = \int_1^P V dP + RT \ell n a$
		$\left(\frac{\partial G}{\partial \ell n X}\right)_{P,T} = RT$	$\bar{G} - G^* = RT \ell n X$	$\bar{G} - G^* = RT \ell n (X\gamma)$	
Liquids Standard state: one molal solution at 1 atm	$\left(\frac{\partial G}{\partial P}\right)_T = V$	$\bar{V}$ of one molal solution $= \bar{V}^\infty$ of real solution	$G^\square - G^\circ = \int_1^P \bar{V}^\infty dP$		$\bar{G} - G^\circ = \int_1^P \bar{V}^\infty dP + RT \ell n a$
		$\left(\frac{\partial \bar{G}}{\partial \ell n m}\right)_{P,T} = RT$	$\bar{G} - G^\square = RT \ell n m$	$\bar{G} - G^\square = RT \ell n (m\gamma)$	

At reaction equilibrium $\Delta G = 0$ and Q is equal to the equilibrium constant K

$$\Delta G^\circ = -RT \ln K - \int_{P=1}^{P} \Delta V dP - \int_{P=1}^{P} \Delta \bar{V}^\infty \, dP$$

The volume change due to solid reactants and products commonly is nearly constant over a large PT range and approximately equal to ΔV_S at 25°C and 1 atmosphere. It is important to note that this is not true for the volume change due to ions. Such volume change may not be too sensitive to pressure differences but varies significantly with temperature.

The Variation of ΔG^0 with Temperature

The heat capacity of a substance in its standard state is commonly expressed by an empirical relationship. A common equation is

$$C_P^\circ = a + bT + cT^{-2}$$

which has a similar form to the equation proposed by Maier and Kelley (1932).

Consequently, ΔC_P° of a reaction is given by

$$\Delta C_P^\circ = \Delta a + \Delta bt + \Delta cT^{-2}$$

Substituting this in the differential equations

$$\left(\frac{\partial \Delta H^\circ}{\partial T}\right)_P = \Delta C_P^\circ \quad \text{and} \quad \left(\frac{\partial \Delta S^\circ}{\partial T}\right)_P = \frac{\Delta C_P^\circ}{T}$$

the following expressions are obtained

$$\Delta H^\circ = \int (\Delta a + \Delta bT + \Delta cT^{-2}) dT$$

$$= \Delta H_I + \Delta aT + \tfrac{1}{2}\Delta bT^2 - \Delta cT^{-1}$$

$$\Delta S^\circ = \int \left(\frac{\Delta a + \Delta bT + \Delta cT^{-2}}{T}\right) dT$$

$$= \Delta S_I + \Delta a \ln T + \Delta bT - \tfrac{1}{2}\Delta cT^{-2}$$

where ΔH_I and ΔS_I are integration constants. (In most texts, ΔH_I is designated as ΔH_0). These relations hold only within the validity range of the heat capacity equation. Substituting these expressions into the formula

$$\Delta G^\circ = \Delta H^\circ - T\Delta S^\circ$$

the following relationship is obtained

$$\Delta G^\circ = \Delta H_I + \Delta aT + \tfrac{1}{2}\Delta bT^2 - \Delta cT^{-1} - \Delta S_I T - \Delta bT^2 + \tfrac{1}{2}\Delta cT^{-1} - \Delta aT \ln T$$

$$\Delta G^\circ = \Delta H_I - T\Delta S_I - \Delta aT \ln T + \Delta aT - \tfrac{1}{2}\Delta bT^2 + \tfrac{1}{2}\Delta cT^{-1}$$

$$\Delta G^\circ = \Delta H_I - T(\Delta S_I - \Delta a) - \Delta aT \ln T - \tfrac{1}{2}\Delta bT^2 - \tfrac{1}{2}\Delta cT^{-1}$$

If heat capacities of all reactants and products are available, two or more measurements of ΔG° at different temperatures make it possible to solve for ΔH_I and ΔS_I. One measurement may be extrapolated to other temperatures if the following information is also available

Either

a. ΔH° at one temperature. This allows to solve for ΔH_I.

or

b. ΔS° at one temperature. This allows to solve for ΔS_I.

For some reactions, ΔC_P° is small and a common approximation is the assumption that $\Delta C_P^\circ = 0$. In this case

$$\Delta G^\circ = \Delta H_I - T\Delta S_I$$

A better approximation is the assumption that ΔC_P° = constant, allowing a nonlinear variation of ΔG° with temperature. In this case

$$\Delta G^\circ = \Delta H_I - T(\Delta S_I - \Delta a) - \Delta aT \ln T$$

Tabulation of Thermochemical Data

Many thermochemical compilations tabulate ΔG° of formation and other properties at temperature intervals. Others, tabulate ΔH° of formation at 25°C, entropy at 25°C, and constants in the heat capacity equation. The fitting of heat capacity data with too many adjustable constants results in a very unstable extrapolation (Day and Halbach, 1979). It is advisable to calculate heat capacities from the five-constant equation in Robie et al. (1978) and refit the data with the three-constant Maier-Kelley equation.

The standard state in most compilations (JANAF, CODATA) is one atmosphere, but in others, e.g. Robie et al. (1978) and Helgeson (1969) the standard state is one bar. Commonly the difference is small but the following formula can be used to covert to the more conventional standard state of one atmosphere

$$\Delta G_f^\circ \text{ (1 atm)} = \Delta G_f^\circ \text{ (1 bar)} + \int_{0.9869}^{1} nRT \ln P$$

where n is the change in the number of gas moles in the reaction which forms one mole of substance from the elements.

Electron Activity

Electrolytes are characterized by the presence of charged species. An electrolyte solution is subject to the constraint of charge neutrality. This makes some measurements impossible and gives rise to difficulties not encountered in dealing with neutral species. For example, the formal definition

$$\bar{G}_{H^+} = \left(\frac{\partial G_{system}}{\partial n_{H^+}}\right)_{Cl^-}$$

does not represent an operation which can be carried out. It turns out that only combinations of the molar free energy of ions can be measured, e.g. $\bar{G}_{H^+} + \bar{G}_{Cl^-}$.

Thermodynamic treatment of electrolytes is made easier by considering the electron as a species present in the solution. One mole of electrons has a partial molar Gibbs free energy ($\bar{G}_e$) in solution that varies with concentration. For all species it is convenient to define a unit-activity state from which to measure energy changes due to composition changes. For aqueous species this commonly is the one-molal hypothetical solution, but this convention is not practical for the electron. Instead the unit activity state of electrons is the state in which they exist in the standard hydrogen electrode, that is, a platinum metal electrode in a hypothetical one-molal H^+ solution and in contact with hydrogen gas at unit fugacity. Like the hypothetical solution, the standard hydrogen electrode does not physically exist (Biegler and Woods, 1973) but is merely a calculation aid.

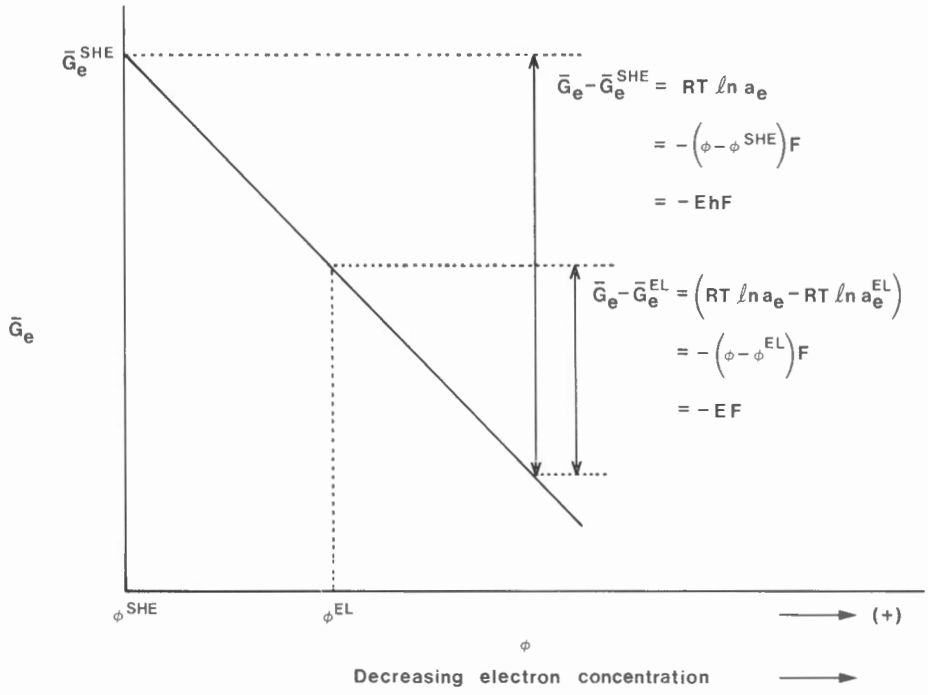

Figure 5. *Definition of electron activity.*

The partial molar Gibbs free energy of one mole of electrons in some other electrode is measured with respect to that in the standard hydrogen electrode (Fig. 5) and the electron activity in the other electrode is defined by this energy difference. The energy difference between two states of one mole of electrons (in the same metal) is given by the difference in electrical potential multiplied by the Faraday constant(F = 23 061 calories/volt-mole)and the electron activity in an electrode with respect to the standard hydrogen electrode (SHE) is given by

$$\bar{G}_e - G_e^{SHE} = RT \ln a_e = -(\phi - \phi^{SHE})\,F$$

The negative sign of the potential differences arises from the negative charge of the electron. The potential difference is measured by an electromotive force E of a galvanic cell combining the two electrodes; if measured with respect to the standard hydrogen electrode it is designated Eh. To be consistent with the sign convention in Garrels and Christ (1965), $(\phi - \phi^{SHE}) = Eh$ when the cell reaction is written so that the electrons in a given electrode appear on the right and the electrons in the hydrogen electrode on the left.

The difference in the logarithms of the electron activity in two electrodes, multiplied by RT, is given by a potential difference or by an electromotive force E multiplied by the Faraday constant (Fig. 5).

Galvanic Cells

Each electrode is characterized by a specific reaction but the individual electrode reactions cannot be measured. However, if two electrodes are combined to form a galvanic cell, the energy change of the combined reaction can be measured. Because of the poor electronic conductivity of water (or some other suitable electrolyte), electrons at different concentrations in the two electrodes can be equilibrated. When the two reactions are added, the electrons cancel out in the mass balance equation, but they do not cancel in the energy balance because the partial molar Gibbs free energy of one mole of electrons, and therefore the electron activity, is different in the two electrodes (Fig. 6). The energy balance of the cell reaction can be analyzed in the usual manner (Fig. 7) by assembling both sides of the reaction equation from the elements, using two energy increments ΔG_f° and RT ln a (there is no VdP term at 1 atmosphere).

$$\Delta G = 0 = \Delta G^\circ - 2\,RT \ln m - RT \ln \gamma_{H^+} - RT \ln \gamma_{Cl^-} + (RT \ln a_e^{CE} - RT \ln a_e^{HE})$$

$$- (RT \ln a_e^{CE} - RT \ln a_e^{HE}) + 2\,RT \ln m = \Delta G^\circ - RT \ln \gamma_{H^+} - RT \ln \gamma_{Cl^-}$$

$$\left(RT\,\ell n\,a_e^{CE} - RT\,\ell n\,a_e^{HE}\right) = -\left(\phi^{CE} - \phi^{HE}\right)F = -EF$$

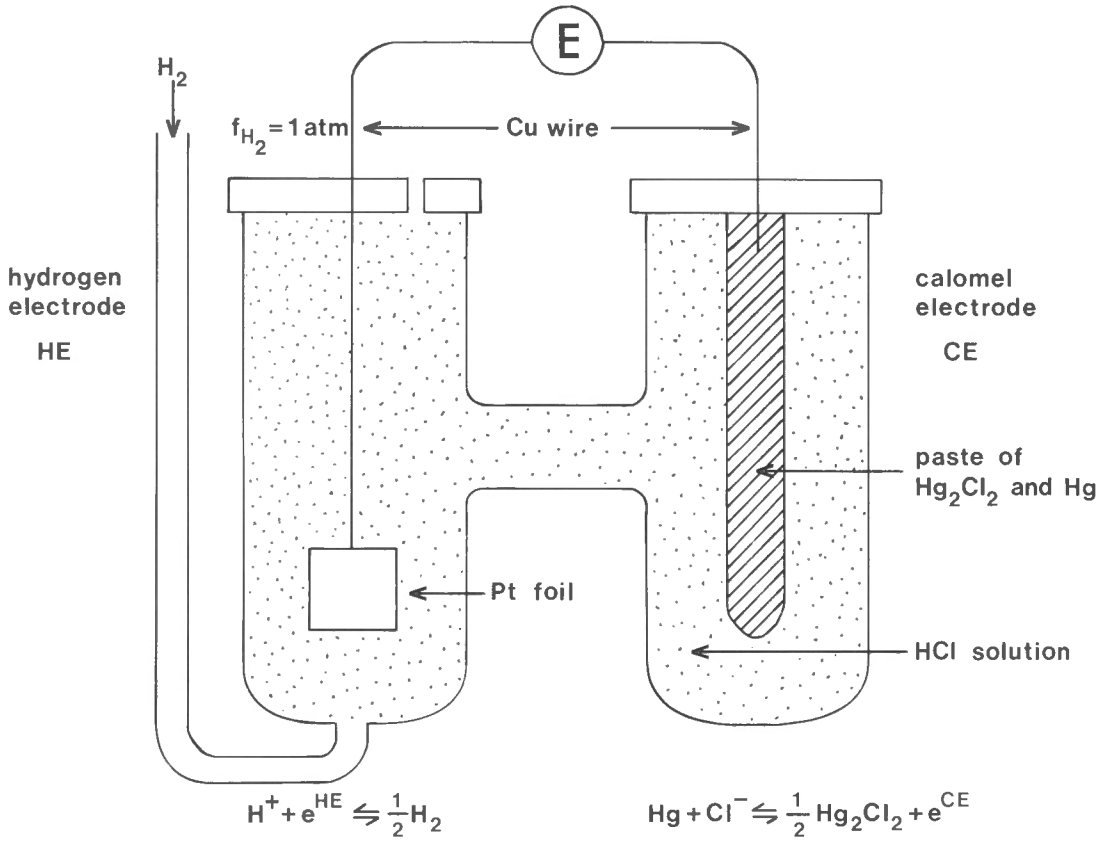

adding the two reactions

$$\left(H^+ + e^{HE}\right) + \left(Cl^- - e^{CE}\right) + Hg \leftrightharpoons \frac{1}{2}Hg_2Cl_2 + \frac{1}{2}H_2$$

Figure 6. *Galvanic cell consisting of a hydrogen electrode and a calomel electrode.*

The electromotive force of this cell can be measured and $-(RT \ln a_e^{CE} - RT \ln a_e^{HE})$ is equal to EF. The molality is also measured and, therefore, the left side of the last equation is known (Table 2). By extrapolation to infinite dilution (zero concentration) $\Delta G°$ is obtained (Fig. 8). The logarithms of activity coefficients become zero at infinite dilution. Empirical observation and later on the Debye-Hückel theory indicated that activity coefficients in electrolytes consisting of one positive and one negative univalent ion vary as $\sqrt{m}$.

The standard Gibbs free energy change of reaction is

$$\Delta G° = -\Delta G_f° \text{ of } (H^+ + e^{SHE}) - \Delta G_f° \text{ of } (Cl^- - e^{SHE}) + \Delta G_f° \text{ of } \tfrac{1}{2} Hg_2Cl_2$$

$$= 6175 \text{ calories}*$$

and, since $\Delta G_f°$ of $\frac{1}{2} Hg_2Cl_2$ is -25 175 calories

$$\Delta G_f° \text{ of } (H^+ + e^{SHE}) + \Delta G_f° \text{ of } (Cl^- - e^{SHE}) = -31\,350 \text{ calories}$$

Hydrogen Ion Convention

The half-reaction of the hydrogen electrode is given by

$$\tfrac{1}{2} H_2 \leftrightharpoons H^+ + e^{HE}$$

$$\Delta G = \Delta G° + RT \ln \left(\frac{a_{H^+}\, a_e}{f_{H_2}^{1/2}} \right)$$

*1 calorie = 4.184 J

Table 2. Experimental data for the cell reaction $(H^+ + e^{HE}) + (Cl^- - e^{CE}) + Hg \leftrightharpoons \frac{1}{2}Hg_2Cl_2 + \frac{1}{2}H_2$ (from Denbigh, 1971)

Molality of HCl	E volts	$-(RT \ln a_e^{CE} - RT \ln a_e^{HE})$ = EF cal	Left side cal	$\sqrt{m}$
0.119304	+0.38948	+8981.4	+6462	0.3454
0.051645	+0.42994	+9914.4	+6403	0.2273
0.0109474	+0.50532	+11652.7	+6306	0.1046
0.0050403	+0.543665	+12536.9	+6268	0.0710
0.0016077	+0.60080	+13854.4	+6231	0.0401

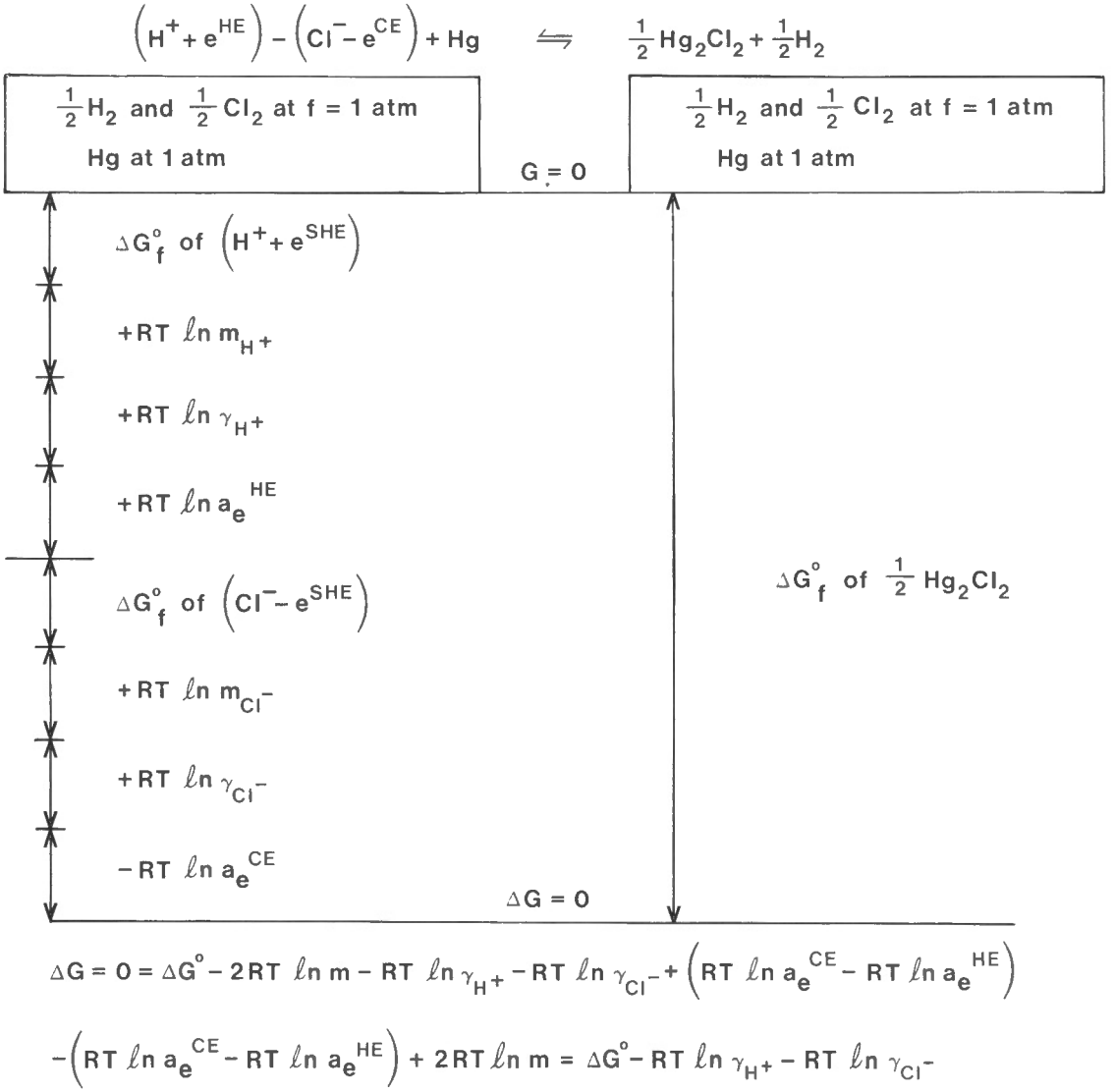

$$\Delta G = 0 = \Delta G^\circ - 2RT \ell n\, m - RT \ell n\, \gamma_{H^+} - RT \ell n\, \gamma_{Cl^-} + \left(RT \ell n\, a_e^{CE} - RT \ell n\, a_e^{HE}\right)$$

$$-\left(RT \ell n\, a_e^{CE} - RT \ell n\, a_e^{HE}\right) + 2RT \ell n\, m = \Delta G^\circ - RT \ell n\, \gamma_{H^+} - RT \ell n\, \gamma_{Cl^-}$$

Figure 7. *The Gibbs free energy change of the reaction in the galvanic cell shown in Figure 6.*

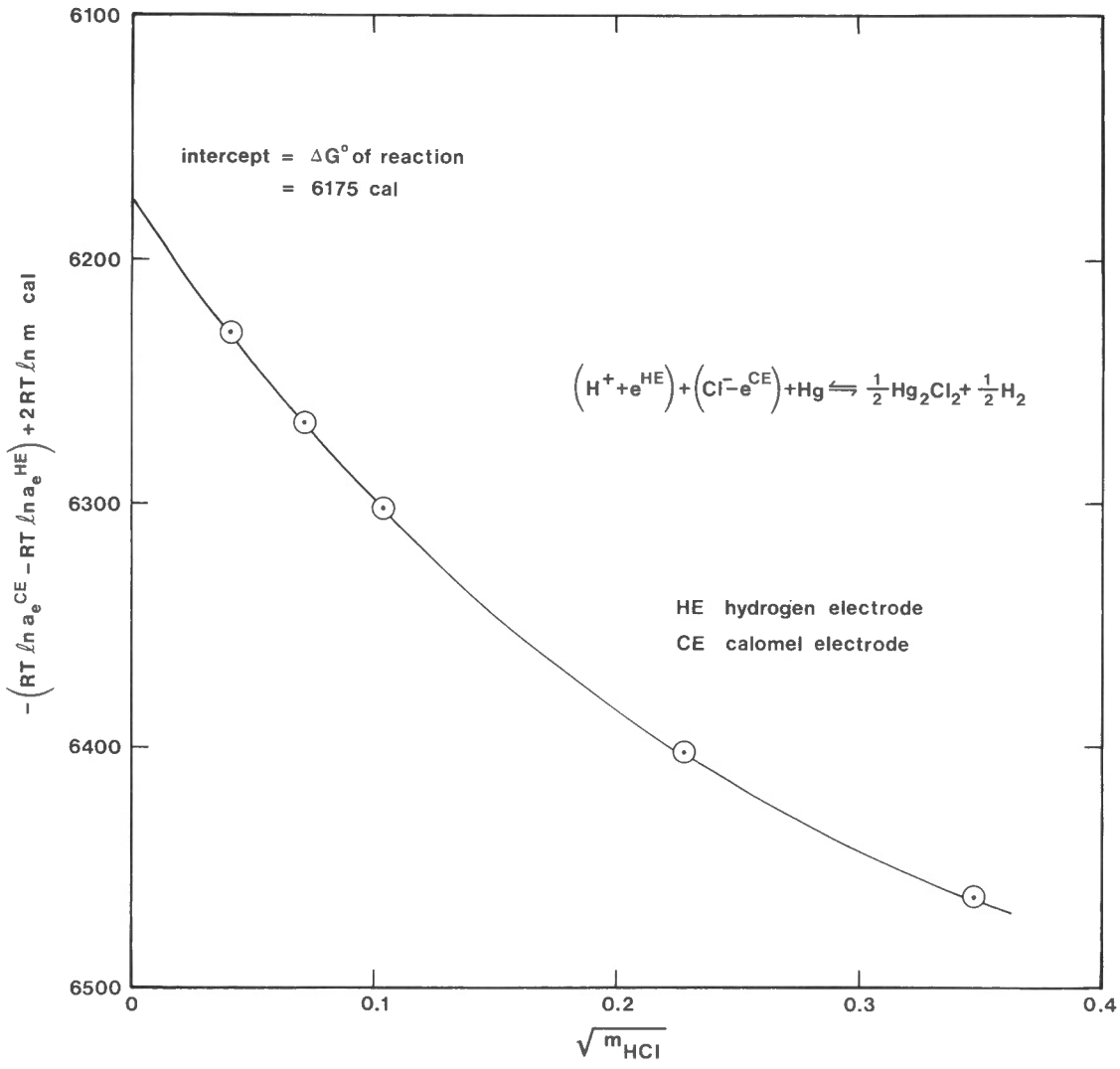

Figure 8. *Determination of the standard Gibbs free energy change of the reaction in the galvanic cell shown in Figure 6.*

By equilibrating species in their standard state (=unit activity state at 1 atmosphere) and having made the assumption that $a_e^{SHE} = 1$

$$\Delta G_f^\circ \text{ of } (H + e^{SHE}) = 0$$

This equation is known as the hydrogen ion convention. In most texts, it is introduced as an assumption but here it follows as a consequence of using the standard hydrogen electrode to define the unit-activity state of electrons. The hydrogen ion convention makes it possible to assign a Gibbs free energy of formation of one mole of each ion, in its standard state, together with the appropriate number of moles of electrons, in their standard state, to maintain charge neutrality.

Thus

$$\Delta G_f^\circ \text{ of } (Cl^- - e^{SHE}) = -31\,350 \text{ calories}$$

Activity Coefficients

If the standard free energy change of a cell reaction has been determined, the cell can be used to measure activity coefficients. In the discussed example, it is possible, at each molality, to solve for the sum $RT \ln \gamma_{H^+} + RT \ln \gamma_{Cl^-}$. This sum can be used to define the mean ionic activity coefficient $\gamma_\pm$

$$RT \ln \gamma_{\pm\ HCl} = (RT \ln \gamma_{H^+} + RT \ln \gamma_{Cl^-}) / 2$$

In calculations, it is very convenient to have individual ionic activity coefficients. Because they cannot be measured, a convention is needed to assign individual portions of the total energy increment measured to each ion. One such convention is to equate γ_{K^+} and γ_{Cl^-} in a pure solution of KCl (Garrels and Christ, 1965), i.e. $\gamma_{K^+} = \gamma_{Cl^-} = \gamma_{\pm KCl}$.

The Debye-Hückel theory provides mean ionic activity coefficients as well as individual ionic activity coefficients. In the latter case, the following equation will be used

$$\log \gamma = - \frac{Az^2 \sqrt{I}}{1+\mathring{a} B \sqrt{I}} + B^{\cdot} I$$

where z is the charge and I the true ionic strength defined by

$$I = \tfrac{1}{2} \sum m_i z_i^2$$

A and B are constants which can be expressed as functions of the temperature, the density, and the dielectric constant of the solvent; Helgeson (1969) listed values to 300°C. The parameter å is derived empirically and can be regarded as being approximately the distance of closest approach of ions. Usually it is necessary to use values of å at 25°C listed in Garrels and Christ (1965).

Helgeson (1969) listed various properties of NaCl solutions because they are of particular importance as metal-carrying media. He derived the mean ionic activity coefficient of NaCl, estimated å and thus calculated $B^{\cdot}$. Although $B^{\cdot}$ refers specifically to NaCl solutions, Helgeson (1969) suggested that this value depends essentially on the co-ordination of water molecules and can be used for other ions, if present in small concentrations compared to that of NaCl.

The activity coefficients of neutral species in electrolyte solutions are approximately equal and commonly it is assumed that they are equal to the activity coefficient of CO_2.

Concentration Cells

In all galvanic cells, the electron activity is different at the two electrodes. It is also possible to construct cells where the activity of another species, in addition to that of electrons, is different. In such cases, it is necessary to retain the additional species when adding the two electrode reactions. This is analogous to the previous procedure of not cancelling the electrons in the energy balance.

One example of a concentration cell is the joining of two hydrogen electrodes with a different hydrogen fugacity for each electrode. Adding the two reactions one obtains:

$$\begin{array}{lll} \text{Right} & H_2 & \leftrightharpoons \quad 2H^+ + 2\,e^- \\ \text{Left} & 2H^+ + 2\,e^- & \leftrightharpoons \quad H_2 \\ \hline & (H_{2,R} - H_{2,L}) & \leftrightharpoons \quad 2(e^-_R - e^-_L) \end{array}$$

For this reaction, ΔG° and $-RT \ln K$ are zero

$$2\,RT \ln \left(\frac{a_{e,R}}{a_{e,L}}\right) - RT \ln \left(\frac{f_{H_2,R}}{f_{H_2,L}}\right) = 0$$

$$RT \ln \left(\frac{f_{H_2,R}}{f_{H_2,L}}\right) = -2\,EF$$

The oxygen fugacity sensor (Sato, 1971) is another example of a concentration cell. Two compartments containing oxygen at different fugacities are separated by a solid electrolyte of ZrO_2-CaO, which conducts $O^=$ ions. Platinum electrodes are attached to two sides of the electrolyte barrier. There are the following reactions:

$$\begin{array}{lll} \text{Right} & 2O^= & \leftrightharpoons \quad O_2 + 4e^- \\ \text{Left} & O_2 + 4\,e^- & \leftrightharpoons \quad 2O^= \\ \hline & -(O_{2,R} - O_{2,L}) & \leftrightharpoons \quad 4(e^-_R - e^-_L) \end{array}$$

Since $\Delta G^\circ = -RT \ln K = O$

$$4\,RT \ln \left(\frac{a_{e,R}}{a_{e,L}}\right) + RT \ln \left(\frac{f_{O_2,R}}{f_{O_2,L}}\right) = O$$

$$RT \ln \left(\frac{f_{O_2,R}}{f_{O_2,L}}\right) = 4\,EF$$

Another type of concentration cell has been used as a sulphur fugacity sensor (Sato, 1971; Schneeberg, 1973). The solid electrolyte AgI, which conducts Ag^+ ions, separates a silver electrode from an electrode of $Ag_{2+x}S$ within a compartment containing sulphur vapour. The following reactions take place:

$$\begin{array}{lll} \text{Right} & 2\,Ag_2S & \leftrightharpoons \quad 4\,Ag^+ + 4\,e^- + S_2 \\ \text{Left} & 4\,Ag^+ + 4\,e^- & \leftrightharpoons \quad 4\,Ag \\ \hline & 2\,Ag_2S & \leftrightharpoons \quad 4\,Ag + S_2 + 4\,(e_R^- - e_L^-) \end{array}$$

For this reaction

$$\Delta G^\circ = -RT \ln K = -RT \ln f_{S_2} - 4\,RT \ln \left(\frac{a_{e,R}}{a_{e,L}} \right) + 2\,RT \ln a_{Ag_2S}$$

$$RT \ln f_{S_2} = 4\,EF - (\Delta G^\circ - 2\,RT \ln a_{Ag_2S})$$

The value of the bracketed term can be obtained by measuring E for a known f_{S_2}. Then, assuming that a_{Ag_2S} does not vary appreciably with f_{S_2}, unknown values of f_{S_2} can be determined by measuring E.

Oxidation in Aqueous Solutions

In aqueous solutions, several variables are related to the oxidizing or reducing nature of the environment, as is apparent from the reaction

$$H_2O \leftrightharpoons 2H^+ + 2e^- + \tfrac{1}{2}O_2$$

For a given activity of water (commonly taken as one) and of the hydrogen ion, either the electron activity or the fugacity of oxygen may be used as a measure of the oxidation state. Commonly the electron activity is converted to Eh by the relation

$$Eh\,F = -RT \ln a_e = 2.303\,RT\,pE$$

However, it has been pointed out (Sillén, 1959; Truesdell, 1968) that it would be more convenient to use $-\log a_e$ or pE as a variable. In this paper, the log f_{O_2} - pH diagram, introduced by Barnes and Kullerund (1961), has been used.

As an example, the oxidation of H_2S to $SO_4^=$ is shown in three equivalent representations, assuming that the activities of the two sulphur species are equal (Fig. 9). The following equation is used to construct the pE - pH diagram:

$$H_2S + 4H_2O \leftrightharpoons 10(H^+ + e^-) + (SO_4^= - 2\,e^-)$$

$$-6540 \qquad -(4\times 56\,690) \qquad 0 \qquad -177\,340$$

The values below the substances are the standard Gibbs free energies of formation at 25°C given by Garrels and Christ (1965); the standard Gibbs free energy change of the reaction is 55 960 calories and log K = -41.02.

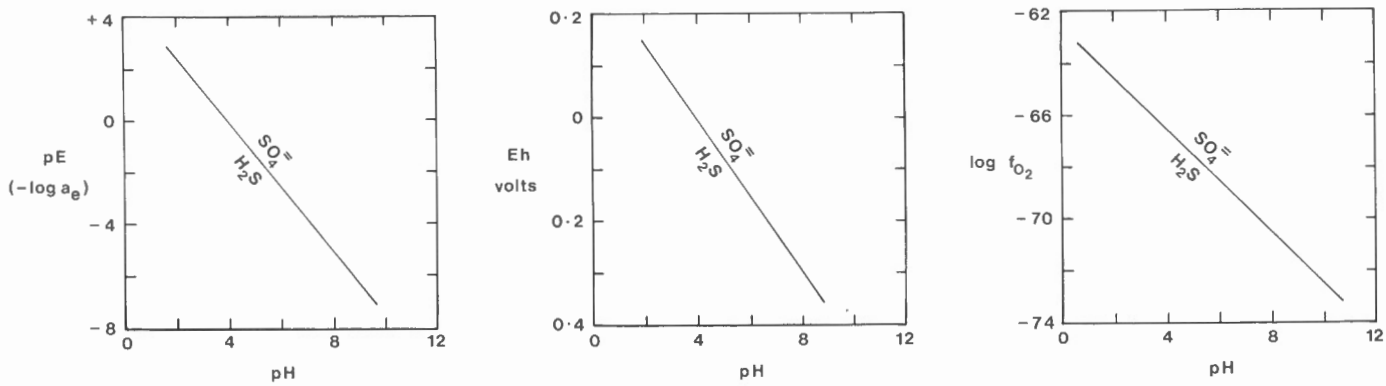

Figure 9. *The oxidation of H_2S to $SO_4^=$ if the activity of the two species is the same.*

Therefore,

$$\log K = -41.02 = 10 \log a_{H^+} + 8 \log a_e$$

$$\log a_e = -\frac{5}{4} \log a_{H^+} - 5.13$$

$$pE = -\frac{5}{4} pH + 5.13$$

The following equation is used to construct the log f_{O_2} - pH diagram:

$$H_2S + 2O_2 \leftrightharpoons 2(H^+ + e^-) + (SO_4^= - 2e^-)$$
$$-6540 \quad 0 \quad 0 \quad -177\,340$$

The free energy change of this reaction is – 170 800 calories and log K = 125.20.

Therefore,

$$\log K = 125.20 = 2 \log a_{H^+} - 2 \log f_{O_2}$$

$$\log f_{O_2} = -pH - 62.60$$

SEDIMENTARY SULPHIDE DEPOSITS

In some sedimentary sulphide deposits, for example the Kupferschiefer, a stratigraphic zonation of metal enrichment in the order Cu-Pb-Zn has been observed (Wedepohl, 1971). In some areas, a diagenetic zonation crosscutting stratigraphy around areas of oxidized rocks is present as well (Rentzsch, 1974). In both cases, the sequence corresponds to a change from more oxidizing to more reducing conditions. According to Rentzsch (1974), the mineral sequence is:

1. hematite
2. chalcocite
3. bornite-chalcocite
4. bornite
5. bornite-chalcopyrite
6. chalcopyrite-pyrite
7. galena-sphalerite-chalcopyrite
8. galena-sphalerite
9. pyrite

Rentzsch discussed this succession in terms of an Eh-pH diagram but the same relations can be presented on a log f_{O_2}-pH diagram. Activity diagrams are constructed from equilibrium constants, listed as such in some publications or obtained from the standard Gibbs free energy change of reactions. The effect of total pressure is insignificant in surface or near-surface deposits.

Predominance Fields of Sulphur Species

The boundaries in Figure 10 are drawn at equal activity of two species; it is not necessary to know the value of the activity, because it cancels out in the equilibrium constant. At 25°C, only three species are important; HSO_4^- is stable only at very low pH and $S^=$ at very high pH. The boundaries between the predominance fields are not phase boundaries; finite concentrations of all species are present at all conditions. However, one species overwhelmingly predominates and the concentration of other species falls off very rapidly away from the boundaries. From Helgeson (1969) the following equilibrium constants, used to plot the boundaries, are obtained:

$H_2S \leftrightharpoons H^+ + HS^-$	log K = -6.99
$H_2S + 2O_2 \leftrightharpoons 2H^+ + SO_4^=$	log K = 125.55
$HS^- + 2O_2 \leftrightharpoons H^+ + SO_4^=$	log K = 132.53

Within the H_2S field, f_{S_2} depends on f_{O_2}, pH, and the activity of the sulphur species. These relations can be seen from the following equations; the equilibrium constants are also from Helgeson (1969):

$2H_2S + O_2 \leftrightharpoons S_2 + 2H_2O$	log K = 59.44
$S_2 + 3O_2 + 2H_2O \leftrightharpoons 4H^+ + 2SO_4^=$	log K = 191.62
$2H^+ + 2HS^- + O_2 \leftrightharpoons S_2 + 2H_2O$	log K = 73.42

By assigning an activity to each sulphur species in its predominance field, it is possible to draw contours of log fS_2. Thus reactions depending on fS_2 can be plotted, e.g. $FeS_2 + \frac{1}{2}S_2 \leftrightharpoons FeS_2$. Alternatively, reactions may be rewritten using f_{O_2}, pH, and sulphur species activity as variables and plotted at a constant value of sulphur species activity. The sulphur concentration in hydrothermal fluids is generally not well known; in many instances it is advisable to draw a series of diagrams for different activities.

Stability Fields of Minerals

The stability boundary of minerals is given by a reaction equation written to involve f_{O_2}, a_{H^+}, and the activity of a sulphur species. The slope of the reaction on a log f_{O_2}-pH diagram follows from the reaction equation (Table 3). In order to locate the boundaries, the co-ordinates of a few points must be determined.

From Robie et al. (1978) the co-ordinates of the triple point pyrite-hematite-magnetite are obtained:

$$6\,Fe_2O_3 \leftrightharpoons 4\,Fe_3O_4 + O_2 \qquad \log K = \log f_{O_2} = -71.10$$

$$FeS_2 + \tfrac{3}{4}O_2 \leftrightharpoons \tfrac{1}{2}Fe_2O_3 + S_2 \qquad \log K = 23.07$$

To the last equation the following equation is added:

$$S_2 + 3O_2 + 2H_2O \leftrightharpoons 4H^+ + 2SO_4^= \qquad \log K = 191.62$$

thus obtaining

$$FeS_2 + \tfrac{15}{4}O_2 + 2H_2O \leftrightharpoons \tfrac{1}{2}Fe_2O_3 + 4H^+ + SO_4^= \qquad \log K = 214.69$$

Assuming that $a_{SO_4^=} = 10^{-6}$ and knowing log f_{O_2}, pH = 9.98

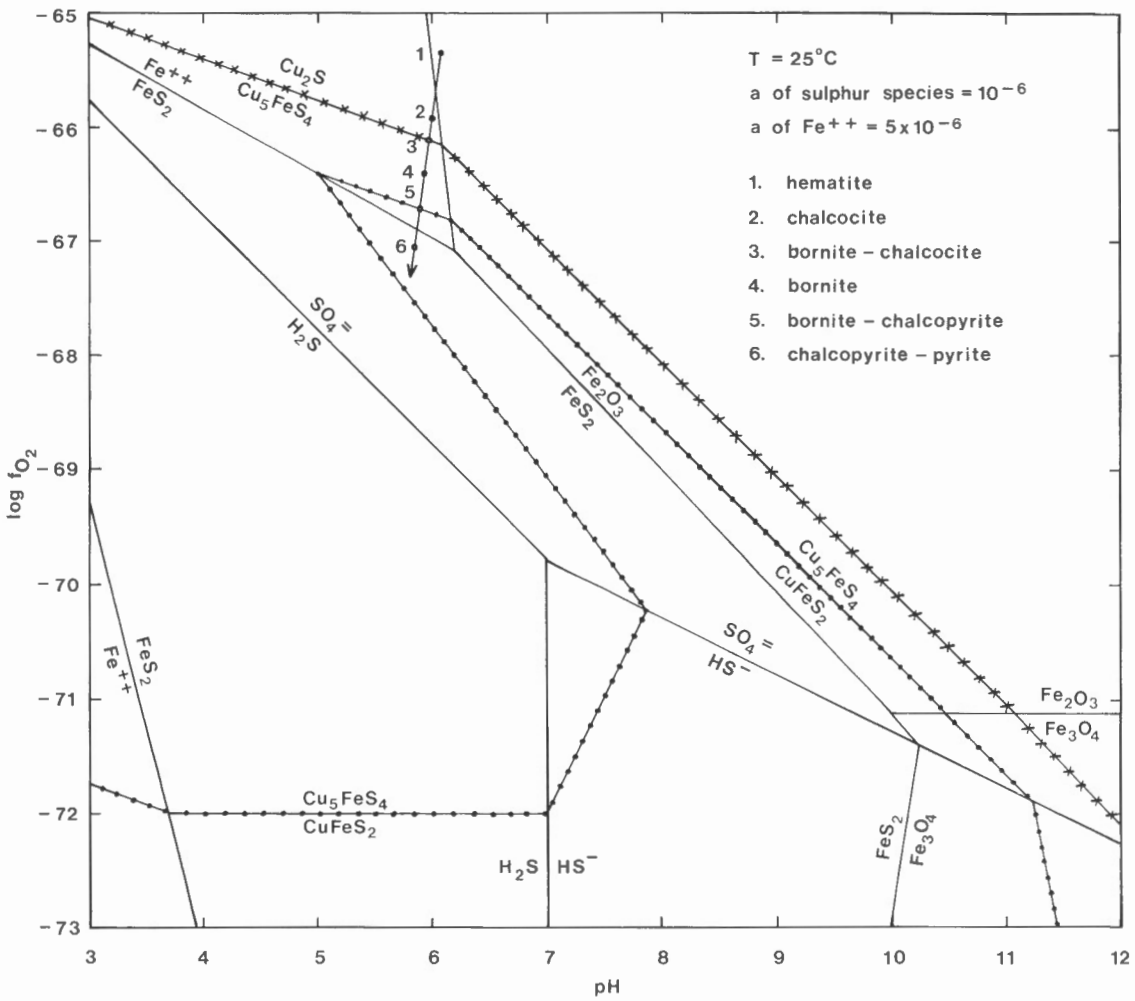

Figure 10. *Mineral stabilities in sedimentary copper deposits.*

Table 3. Reaction equations used in constructing Figure 10

	Slope
$Fe_3O_4 + 6H^+ + 6HS^- + O_2 \leftrightharpoons 3FeS_2 + 6H_2O$	6:1
$3FeS_2 + 11O_2 + 6H_2O \leftrightharpoons Fe_3O_4 + 12H^+ + 6SO_4^=$	-12:11
$3Fe_2O_3 \leftrightharpoons 2Fe_3O_4 + \frac{1}{2}O_2$	0
$Fe_2O_3 + 8H^+ + 4SO_4^= \leftrightharpoons 2FeS_2 + \frac{15}{2}O_2 + 4H_2O$	-16:15
$Fe_2O_3 + 4H^+ \leftrightharpoons 2Fe^{++} + 2H_2O + \frac{1}{2}O_2$	-8:1
$FeS_2 + 2H^+ + \frac{17}{2}O_2 \leftrightharpoons Fe^{++} + \frac{1}{2}H_2O + 2SO_4^=$	-4:7
$FeS_2 + 2H^+ + H_2O \leftrightharpoons Fe^{++} + 2H_2S + \frac{1}{2}O_2$	-4:1
$Cu_5FeS_4 + 4FeS_2 + 2H_2O \leftrightharpoons 5CuFeS_2 + 2H_2S + O_2$	0
$Cu_5FeS_4 + 4FeS_2 + 2H_2O \leftrightharpoons 5CuFeS_2 + 2HS^- + 2H^+ + O_2$	2:1
$Cu_5FeS_4 + 4FeS_2 + 2H_2O + 3O_2 \leftrightharpoons 5CuFeS_2 + 2SO_4^= + 4H^+$	-4:3
$Cu_5FeS_4 + 4Fe^{++} + 6SO_4^= + 4H^+ \leftrightharpoons 5CuFeS_2 + 2H_2O + 11O_2$	-4:11
$Cu_5FeS_4 + 2Fe_2O_3 + 6SO_4^= + 12H^+ \leftrightharpoons 5CuFeS_2 + 6H_2O + 12O_2$	-1:1
$Cu_5FeS_4 + \frac{4}{3}Fe_3O_4 + 6SO_4^= + 12H^+ \leftrightharpoons 5CuFeS_2 + 6H_2O + \frac{35}{3}O_2$	-36:35
$Cu_5FeS_4 + HS^- + 3H_2O + \frac{4}{3}Fe_3O_4 + 6H^+ \leftrightharpoons 5CuFeS_2 + 6H_2O + \frac{7}{6}O_2$	-36:7
$2Cu_5FeS_4 + H_2O + \frac{11}{2}O_2 \leftrightharpoons 5Cu_2S + 3SO_4^= + 2Fe^{++} + 2H^+$	-4:11
$2Cu_5FeS_4 + 3H_2O + 6O_2 \leftrightharpoons 5Cu_2S + Fe_2O_3 + 3SO_4^= + 6H^+$	-1:1
$2Cu_5FeS_4 + 3H_2O + \frac{35}{6}O_2 \leftrightharpoons 5Cu_2S + \frac{2}{3}Fe_3O_4 + 3SO_4^= + 6H^+$	-36:35

In a similar fashion the co-ordinates of the point pyrite-hematite-solution with $a_{Fe^{++}} = 5 \times 10^{-6}$ are determined, again using data from Robie et al. (1978):

$$FeS_2 + \tfrac{1}{2}Fe_2O_3 + \tfrac{13}{4}O_2 \leftrightharpoons 2Fe^{++} + 2SO_4^= \qquad \log K = 195.42$$

$$Fe_2O_3 + 4H^+ \leftrightharpoons 2Fe^{++} + 2H_2O + \tfrac{1}{2}O_2 \qquad \log K = 19.39$$

Assuming that $a_{SO_4^=} = 10^{-6}$ and $a_{Fe^{++}} = 5 \times 10^{-6}$ (Rentzsch, 1974) it follows that $\log f_{O_2} = -67.08$ and pH = 6.19.

The chalcopyrite-bornite boundary in the pyrite field is obtained by risking an extrapolation of the higher temperature data of Schneeberg (1973) and adding his reaction to the reaction relating f_{S_2} to a_{H_2S}:

$$Cu_5FeS_4 + 4FeS_2 \leftrightharpoons 5CuFeS_2 + S_2 \qquad \log K = -24.56$$

$$S_2 + 2H_2O \leftrightharpoons 2H_2S + O_2 \qquad \log K = -59.44$$

$$Cu_5FeS_4 + 4FeS_2 + 2H_2O \leftrightharpoons 5CuFeS_2 + 2H_2S + O_2 \qquad \log K = -84.00$$

If $a_{H_2S} = 10^{-6}$, $\log f_{O_2} = -72.00$

In order to plot the chalcocite-bornite boundary, the equilibrium constant for the reaction below is calculated, using standard Gibbs free energy values from Robie et al. (1978), except taking the standard Gibbs free energy of formation of bornite from Helgeson (1969):

$$2Cu_5FeS_4 + 3H_2O + 6O_2 \leftrightharpoons 5Cu_2S + Fe_2O_3 + 3SO_4^= + 6H^+ \qquad \log K = 342.46$$

Comments

The diagram shown in Figure 10 adequately portrays the first six mineral assemblages in the observed zonation. Rentzsch (1974) pointed out that the chalcocite mineralization is associated with iron-poor rocks. In the oxidized rocks, early diagenetic pyrite was converted to hematite and some iron might have been removed in solution. It is important to note that only in the hematite field or in the Fe^{++} solution field does reduction lead to the sequence chalcocite-bornite-chalcopyrite. Within the pyrite field, further reduction would cause the appearance of bornite.

LOW TEMPERATURE LEAD-ZINC DEPOSITS

In many sedimentary basins, galena and sphalerite occur as open-space fillings in a carbonate host rock. Although deposition took place after lithification, the mineralization is commonly confined to certain strata. Typical examples of this class of deposits are those of the Mississippi Valley. From the study of fluid inclusions (Roedder, 1967), it has been deduced that the ores were deposited from sulphate-bearing brines at temperatures of 80-150°C. It has been suggested that such brines originate during diagenesis (Jackson and Beales, 1967). Anderson (1975) proposed that the metals were carried as chloride complexes and precipitation could be caused by cooling, dilution, increasing pH, and reduction. The last two effects can be conveniently shown on a log f_{O_2}- pH diagram (Anderson, 1973, 1975). Following Anderson (1977), a minimum concentration of log m = -5 will be accepted for a potential ore-forming fluid; this is equivalent to about 2 ppm Pb and 0.3 ppm H_2S.

The Solubility of Galena

The predominance fields of the sulphur species (Fig. 11) can be plotted from the equilibrium constants at 100°C (Helgeson, 1969):

$$H_2S \leftrightharpoons H^+ + HS^- \qquad \log K = -6.63$$

$$H_2S + 2O_2 \leftrightharpoons 2H^+ + SO_4^= \qquad \log K = 94.31$$

$$HS^- + 2O_2 \leftrightharpoons H^+ + SO_4^= \qquad \log K = 100.93$$

For a neutral species like H_2S, the activity coefficient is assumed to be equal to that of CO_2 which is 1.74 in a 3 m NaCl solution at 100°C, (Helgeson, 1969). Thus if log m_{H_2S} = -5, log a_{H_2S} = -4.76; this activity has also been assumed for the other sulphur species. In the H_2S field, the following equilibrium holds:

$$PbS + 2H^+ \leftrightharpoons Pb^{++} + H_2S \qquad \log K = -5.57 \text{ (Helgeson, 1969)}$$

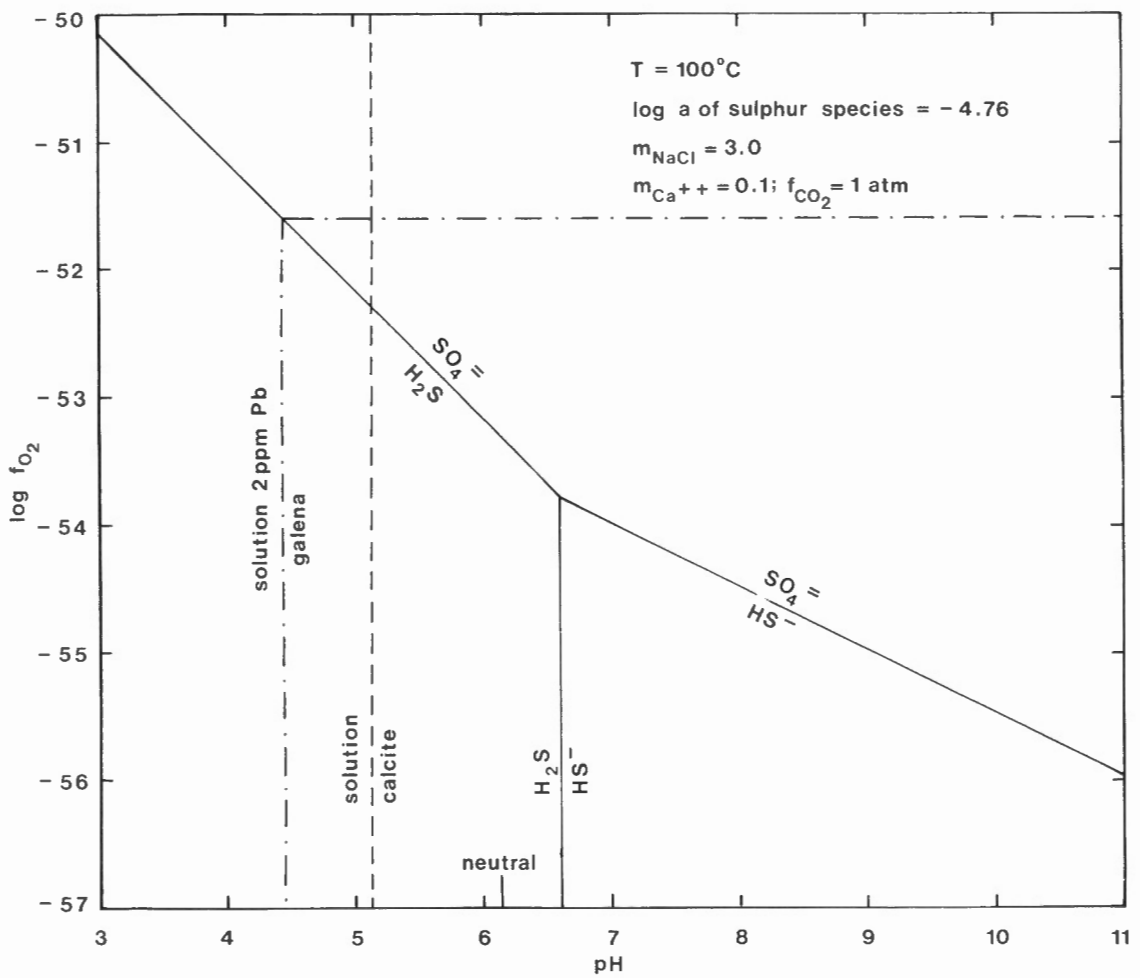

Figure 11. *The solubility of galena at 100°C.*

The following concentration ratio, valid in 3 m NaCl solutions, can be calculated from the equations given by Anderson (1973):

$$\log m_{PbCl_4^{=}} - \log (m_{Pb^{++}} \; m^4_{Cl^-}) = 3.21$$

In concentrated solutions, $PbCl_4^{=}$ constitutes more than 85 per cent of the dissolved lead (Nriagu and Anderson, 1971). Thus if it is assumed that log $m_{PbCl_4^{=}} = -5$, then log $m_{Pb^{++}} = -8.69$ which must in turn be converted into activity. The activity coefficient can be calculated from the Debye-Hückel equation. The constants A,B, and B° are given by Helgeson (1969). The value å is not known at 100°C; therefore, the value å at 25°C from Garrels and Christ (1965) was used as an approximation. The value of log $\gamma_{Pb^{++}}$ was found to be -1.00; therefore, log $a_{Pb^{++}} = -9.69$. For these conditions, pH = 4.44 and the log $m_{PbCl_4^{=}} = -5$ (log $a_{Pb^{++}} = -9.69$) contour can be plotted. It will intersect the H_2S - $SO_4^{=}$ boundary giving rise to the reaction

$$PbS + 2O_2 \leftrightharpoons Pb^{++} + SO_4^{=}$$

which plots as a horizontal line in Figure 11.

Comments

It is seen that, in a highly reduced solution, lead could be transported only at very low pH. In carbonate rocks such low values cannot be maintained. Calcite stability is governed by the equilibrium $CaCO_3 + 2H^+ \leftrightharpoons Ca^{++} + H_2O + CO_2$(gas) for which log K = 9.25 (Helgeson, 1969). If f_{CO_2} = 1 atmosphere and $a_{Ca^{++}} = 0.1$, then pH = 5.13. At this pH, the brine could carry appreciable amounts of lead only at oxidizing conditions. Precipitation would have to be caused either by reduction at the site of deposition or, as suggested by Jackson and Beales (1967) by mixing of brine with H_2S-rich solutions present in limestones.

VOLCANOGENIC SULPHIDE DEPOSITS

In volcanic terranes, stratiform lenses of massive sulphides occur along stratigraphic horizons. It is now generally accepted that the sulphides are chemical precipitates deposited on the sea floor. The metals presumably were supplied by hot saline solutions which reached the surface as hot springs. An alteration zone is present below sulphide bodies deposited near the vent (Roscoe, 1965). The outstanding feature of the alteration process is the decomposition of feldspars and Ca-bearing minerals resulting in rocks depleted in Na and Ca. At low grades, altered mafic rocks would be chlorite-rich but in metamorphic terranes they may occur as cordierite-anthophyllite rocks (Froese, 1969; Whitmore, 1969). Felsic volcanic rocks are chloritized as well, the necessary Fe and Mg apparently being available in the mineralizing solutions. The sulphide deposits are typically zoned from a Cu-rich base to a Zn-rich top. These features of volcanogenic sulphide deposits will be examined in terms of a log f_{O_2} - pH diagram at 300°C, essentially following Large (1977).

Stability Fields of Iron Oxides and Sulphides

In Figure 12 the predominance fields of the sulphur species were drawn from the following equilibrium constants given by Helgeson (1969):

1) $HSO_4^- \leftrightharpoons H^+ + SO_4^{=}$	log K = 7.06
2) $H_2S \leftrightharpoons H^+ + HS^-$	log K = 8.06
3) $H_2S + 2O_2 \leftrightharpoons H^+ + HSO_4^-$	log K = 55.61
4) $H_2S + 2O_2 \leftrightharpoons 2H^+ + SO_4^{=}$	log K = 48.55
5) $HS^- + 2O_2 \leftrightharpoons H^+ + SO_4^{=}$	log K = 56.61

The boundaries between stability fields of minerals are given by appropriate reactions; the slope of each boundary on a log f_{O_2}-pH diagram follows from the reaction equation (Table 4). In order to locate the boundary, the co-ordinates of some points must be determined. By adding two reactions

$3Fe + 2O_2 \leftrightharpoons Fe_3O_4$	log K = 83.88	Robie et al. (1978)
$3FeS \leftrightharpoons 3Fe + \frac{3}{2}S_2$	log K = -32.94	Toulmin and Barton (1964)

the following reaction is obtained:

$$3FeS + 2O_2 \leftrightharpoons Fe_3O_4 + \frac{3}{2}S_2 \qquad \log K = 50.94$$

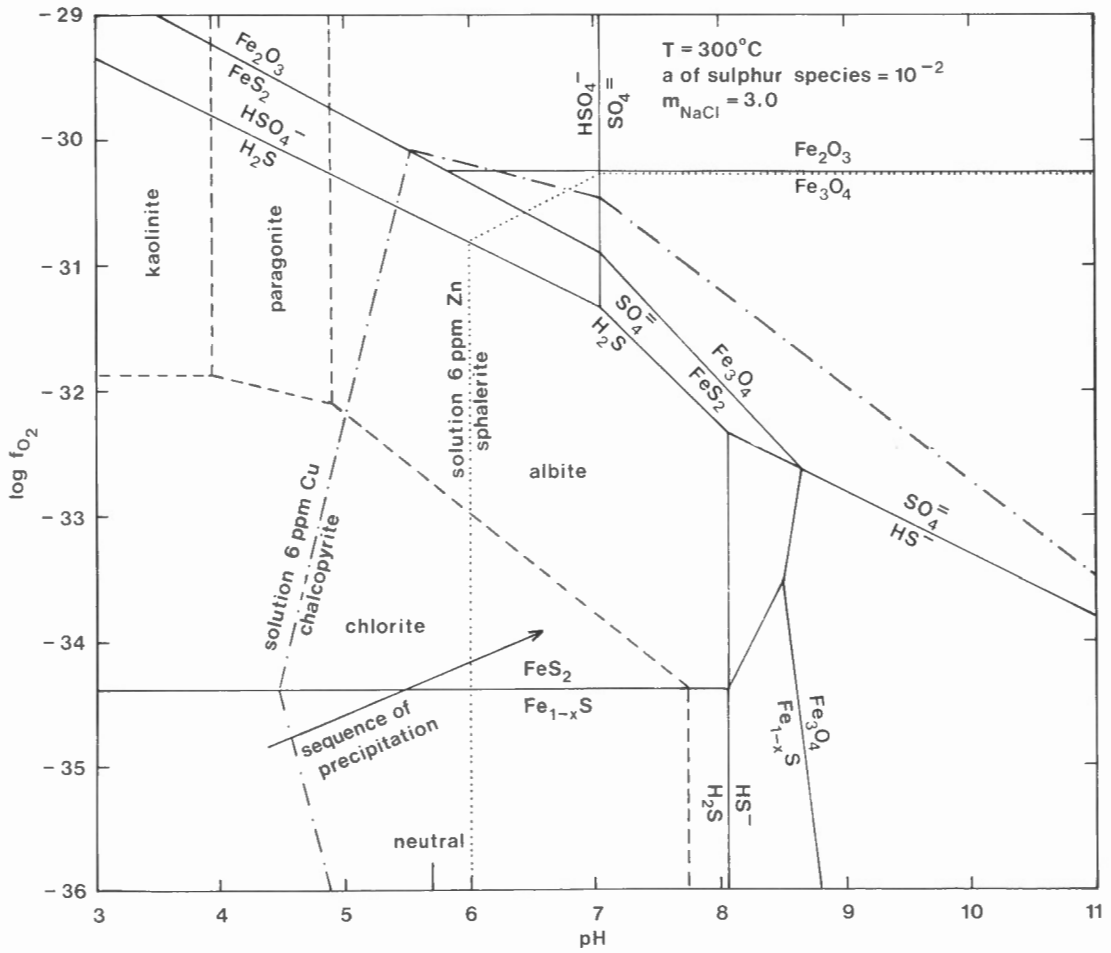

Figure 12. *Mineral stabilities in volcanogenic sulphide deposits.*

Toulmin and Barton (1964) have given equations relating pyrrhotite composition to a_{FeS} and log f_{S_2}. For 300°C, values are listed below.

N_{FeS}	a_{FeS}	log f_{S_2}	log f_{O_2}	log a_{H^+}
0.97	0.804	-14.75	-36.39	-8.85
0.96	0.700	-13.08	-35.06	-8.68
9.9475#	0.565	-11.16	-33.48	-8.51

#coexisting with pyrite.

For a given pyrrhotite composition, a_{FeS} and log f_{S_2} are known and thus log f_{O_2} may be calculated. Assuming a given activity of HS^-, e.g. 10^{-2}, the magnetite-pyrrhotite boundary and the pyrite-pyrrhotite-magnetite triple point may be plotted as follows. Values of f_{S_2} and f_{O_2} are substituted into the equation

$$2H^+ + 2HS^- + O_2 \leftrightarrows S_2 + 2H_2O \qquad \log K = 43.33 \text{ (Helgeson, 1969)}$$

which is then solved for pH (= -log a_{H^+}).

In order to obtain the hematite-magnetite-pyrite triple point, it is necessary to find the intersection of the magnetite-pyrite boundary in the HSO_4^- field with the reaction

$$6Fe_2O_3 \leftrightarrows 4Fe_3O_4 + O_2 \qquad \log f_{O_2} = -30.25 \text{ (Robie et al., 1978)}$$

Table 4. Reaction equations used in constructing Figure 12

	Slope
$2FeS + 2H_2S + O_2 \leftrightharpoons 2FeS_2 + 2H_2O$	0
$2H^+ + 2HS^- + 2FeS + O_2 \leftrightharpoons 2FeS_2 + H_2O$	2:1
$Fe_3O_4 + 6H^+ + 6HS^- + O_2 \leftrightharpoons 3FeS_2 + 6H_2O$	6:1
$3FeS_2 + 11O_2 + 6H_2O \leftrightharpoons Fe_3O_4 + 12H^+ + 6SO_4^=$	-12:11
$3FeS_2 + 11O_2 + 6H_2O \leftrightharpoons Fe_3O_4 + 6H^+ + 6HSO_4^-$	6:11
$6Fe_2O_3 \leftrightharpoons 4Fe_3O_4 + O_2$	0
$Fe_2O_3 + 4H^+ + 4HSO_4^- \leftrightharpoons 2FeS_2 + \frac{15}{2} O_2 + 4H_2O$	-8:15
$CuFeS_2 + H^+ + Cl^- + \frac{1}{2}H_2O \leftrightharpoons H_2S + FeS + \frac{1}{4}O_2 + CuCl$	-4:1
$CuFeS_2 + H^+ + \frac{1}{4}O_2 + Cl^- \leftrightharpoons FeS_2 + \frac{1}{2}H_2O + CuCl$	4:1
$CuFeS_2 + Cl^- + 4O_2 + \frac{3}{2} H_2O \leftrightharpoons \frac{1}{2}Fe_2O_3 + H^+ + 2HSO_4^- + CuCl$	-1:4
$CuFeS_2 + \frac{47}{12} O_2 + Cl^- + \frac{3}{2} H_2O \leftrightharpoons \frac{1}{3} Fe_3O_4 + 2HSO_4^- + H^+ + CuCl$	-12:47
$CuFeS_2 + \frac{47}{12} O_2 + Cl^- + \frac{3}{2} H_2O \leftrightharpoons \frac{1}{3} Fe_3O_4 + 2SO_4^= + 3H^+ + CuCl$	-36:47
$ZnS + 4Cl^- + 2H^+ \leftrightharpoons ZnCl_4^= + H_2S$	∞
$ZnS + H^+ + 4Cl^- + 2O_2 \leftrightharpoons ZnCl_4^= + HSO_4^-$	1:2
$ZnS + 4Cl^- + SO_2 \leftrightharpoons ZnCl_4^= + SO_4^=$	0
$Al_2Si_2O_5(OH)_4 + 5FeS_2 + 12H_2O + SiO_2 \leftrightharpoons (Fe_5Al)Si_3AlO_{10}(OH)_8 + 10H_2S + \frac{5}{2} O_2$	0
$2NaAl_2Si_3AlO_{10}(OH)_2 + 15FeS_2 + 2H^+ + 39H_2O + 3SiO_2 \leftrightharpoons 3(Fe_5Al)Si_3AlO_{10}(OH)_8 + 30H_2S + 2Na^+ + \frac{15}{2}O_2$	-4:15
$2NaAlSi_3O_8 + 5FeS_2 + 2H^+ + 13H_2O \leftrightharpoons (Fe_5Al)Si_3AlO_{10}(OH)_8 + 2Na^+ + 10H_2S + 3SiO_2 + \frac{5}{2} O_2$	-4:5
$2NaAlSi_3O_8 + 5FeS + 2H^+ + 8H_2O \leftrightharpoons (Fe_5Al)Si_3AlO_{10}(OH)_8 + 2Na^+ + 5H_2S + 3SiO_2$	∞

Solubility of Chalcopyrite and Sphalerite

In discussing the stability of iron oxides and sulphides, dissolution has not been considered as a limitation on mineral stabilities, i.e. the solution could maintain a sufficiently high concentration of Fe^{++} to stabilize the oxides and sulphides. In discussing the transport of metals by solutions, it is of some interest to consider the stability of chalcopyrite and sphalerite as restricted by solubility; these minerals are shown as unstable below a minimum concentration of metals. Because minerals commonly dissolve incongruently, i.e. as ions, solubility is best described by a reaction equation or a set of reaction equations.

At 300°C practically all dissolved copper exists in the form of CuCl and, in the pyrite field, the solubility of chalcopyrite is given by the reaction:

$$CuFeS_2 + H^+ + \tfrac{1}{4} O_2 + Cl^- \leftrightharpoons FeS_2 + \tfrac{1}{2}H_2O + CuCl \quad \log K = 9.8$$

The equilibrium constant has been taken from Crerar and Barnes (1976); it can be expressed as:

$$\log K = \log m_{CuCl} + \log \gamma_{CuCl} - \log a_{H^+} - \tfrac{1}{4}\log f_{O_2} - \log m_{Cl^-} - \log \gamma_{Cl^-}$$

A 3 m NaCl solution with 6 ppm Cu, corresponding to 10^{-4}m CuCl, will be considered. According to Helgeson (1969) such a solution contains 34 per cent associated NaCl; therefore, the molality of dissociated NaCl is 0.66 x 3 = 1.98 m. In order to maintain charge balance, it is assumed that $m_{Na^+} = m_{Cl^-}$, all other species having a much lower concentration. It is common practice to equate γ of neutral species to γ of CO_2 in NaCl solutions; from Helgeson (1969), $\gamma_{CO_2} = 2.29 = \gamma_{CuCl}$. The activity coefficient of Cl^- is calculated from the Debye-Hückel equation. Constants A,B, and B° are given in Helgeson (1969). From Garrels and Christ (1965), a value of $\mathring{a} = 3.0 \times 10^{-8}$ at 25°C has been used, because no value is available at 300°C. The result is $\log \gamma_{Cl^-} = -0.678$. Substituting values of m_{CuCl}, γ_{CuCl}, m_{Cl^-}, and γ_{Cl^-} into the equilibrium constant equation, the following relationship is obtained:

$$\tfrac{1}{4}\log f_{O_2} = -13.06 + pH$$

This function can be plotted and the 10^{-4} molality contour can be extended by using appropriate reaction slopes (Table 4).

In very alkaline solutions, the formation of bisulphide complexes increases the solubility of chalcopyrite. A stability limit of chalcopyrite can be calculated from available data for a given activity of a complex. Three equations are added to obtain a convenient relationship:

$$Cu_5FeS_4 + 3\,FeS_2 + \tfrac{3}{2}\,H_2O \leftrightharpoons 4CuFeS_2 + \tfrac{3}{4}\,O_2 + H^+ + Cu(HS)_2^- \qquad \log K = -35 \quad \text{Crerar and Barnes (1976)}$$

$$5CuFeS_2 + S_2 \leftrightharpoons 4FeS_2 + Cu_5FeS_4 \qquad \log K = 6.67 \quad \text{Schneeberg (1973)}$$

$$FeS_2 + \tfrac{2}{3}\,O_2 \leftrightharpoons \tfrac{1}{3}\,Fe_3O_4 + S_2 \qquad \log K = 11.16 \quad f_{O_2} \text{ and } f_{S_2} \text{ at triple point}$$

$$CuFeS_2 + \tfrac{3}{2}\,H_2O \leftrightharpoons \tfrac{1}{3}\,Fe_3O_4 + \tfrac{1}{12}\,O_2 + H^+ + Cu(HS)_2^- \qquad \log K = -17.17$$

For a $Cu(HS)_2^- = 10^{-4}$, pH = 10.42 at log f_{O_2} = -33 and pH = 10.17 at log f_{O_2} = -36. Although bisulphide complexes become more significant at lower temperatures (Crerar and Barnes, 1976), they are not effective transporting agents in the temperature range of hydrothermal solutions responsible for volcanogenic deposits.

At 300°C nearly all zinc exists in the form of $ZnCl_4^=$ (Helgeson, 1969) and the solubility of sphalerite is given by the equation

$$ZnCl_4^= + SO_4^= \leftrightharpoons 4Cl^- + ZnS + 2O_2 \qquad \log K = -54.39 \quad \text{(Helgeson, 1969)}$$

A 6 ppm Zn solution corresponds to 10^{-4} molal. The activity coefficient of $ZnCl_4^=$ is calculated from the Debye-Hückel equation, assuming that $\mathring{a}_{ZnCl_4^=} = \mathring{a}_{Zn^{++}}$; this value is equal to 6.0 x 10^{-8} (Garrels and Christ, 1965). The result is log $\gamma_{ZnCl_4^=}$ = -1.67. It is now possible to solve for log f_{O_2} = -30.27. The 10^{-4} molality contour is completed by using slopes from the reaction equations (Table 4).

Stability of Silicates

The stability fields of albite, paragonite, and kaolinite may be calculated from the following equilibrium constants at 1 kilobar* taken from Montoya and Hemley (1975):

$$1.5\,NaAlSi_3O_8 + H^+ \leftrightharpoons 0.5\,NaAl_2Si_3AlO_{10}(OH)_2 + 3\,SiO_2 + Na^+ \qquad \log K = 4.638$$

$$NaAl_2Si_3AlO_{10}(OH)_2 + H^+ + 1.5\,H_2O \leftrightharpoons 1.5\,Al_2Si_2O_5(OH)_4 + Na^+ \qquad \log K = 3.675$$

The values at 1 atmosphere should not vary much from those at 1 kilobar. In a 3 m NaCl solution, the molality of Na^+ is 0.66 x 3 = 1.98. The activity coefficient of Na^+ can be calculated from the Debye-Hückel equation using $\mathring{a}$ = 4.0 (Garrels and Christ, 1965). The result is γ_{Na^+} = 0.275, from which a_{Na^+} = 0.545. Now pH can be calculated; the values are 4.90 and 3.94, respectively, limiting the stability fields of albite, paragonite, and kaolinite.

The slopes of reactions limiting the stability field of chlorite follow from the reaction equations (Table 4) but since equilibrium constants are not available, the location of the boundaries of the chlorite field is not known. The estimated stability of chlorite is shown for a particular composition of chlorite, which will be affected by the activity of Mg^{++}.

Comments

The precipitation of sulphides takes place near the rock-water interface in a gradient of decreasing temperature and Cl^- concentration and increasing f_{O_2} and pH. In Figure 12, only the path with respect to f_{O_2} and pH can be shown. It is seen that chalcopyrite will precipitate closest to the vent, capped and surrounded by sphalerite-rich ore. Thus differences in solubility will give rise to stratigraphic zoning. Gradients in temperature and Cl^- concentration do not change the relative solubility of Cu and Zn. Plagioclase is not stable in ore-bearing solutions. Na^+ (and Ca^{++}) is removed giving rise to a chlorite ± kaolinite rock, a suitable protolith for cordierite-anthophyllite rocks.

* 1 kilobar = 10^5 kPa

PORPHYRY COPPER DEPOSITS

Copper mineralization occurring as veinlets and disseminations in felsic intrusions is commonly associated with a characteristic alteration of the host rock. Lowell and Guilbert (1970) recognized four alteration zones from the most mineralized portions outward – 1. potassic (biotite, K feldspar) 2. phyllic (sericite) 3. argillic (kaolinite) 4. propylitic (chlorite, epidote, calcite). The copper mineralization is restricted to the potassic alteration zone, whereas the phyllic zone is marked by the presence of abundant pyrite. The other two zones will not be considered here. The log f_{O_2}- pH diagram at 300°C, previously presented, will be used to examine phase relations among minerals. In addition, the stability fields of muscovite, K feldspar, and biotite will be shown.

The Hydrolysis of K Feldspar

Hemley (1959), Shade (1968, 1974), and Montoya and Hemley (1975) investigated the equilibrium

$$1.5\ KAlSi_3O_8 + H^+ \leftrightharpoons 0.5\ KAl_2Si_3AlO_{10}(OH)_2 + 3SiO_2 + K^+$$

at temperatures above 400°C, in KCl-HCl solutions. The concentrations of OH^- and KOH and an amount of a_{H^+} equivalent to a_{OH^-} can be neglected. In such a case, the following relationships hold:

$$K_{KCl} = \left(\frac{a_{K^+}\, a_{Cl^-}}{a_{KCl}}\right)$$

$$K_{HCl} = \left(\frac{a_{H^+}\, a_{Cl^-}}{a_{HCl}}\right)$$

$$a_{K^+} = a_{Cl^-}$$

$$\Sigma H = a_{H^+} + a_{HCl}$$

$$\Sigma K = a_{K^+} + a_{KCl}$$

The concentration of Σ K was kept constant at 2 m and Σ H was determined experimentally. The following calculations can be made, assuming that a = m for all species.

$$\text{Let } X = a_{K^+} = a_{Cl^-}$$

$$K_{KCl} = \left(\frac{a_{K^+}\, a_{Cl^-}}{a_{KCl}}\right) = \frac{X^2}{\Sigma K - X}$$

$$X^2 + X \cdot K_{KCl} - \Sigma K \cdot K_{KCl} = 0$$

This quadratic equation can be solved for X. Knowing Σ H and a_{Cl^-} the equation

$$\Sigma H = a_{H^+} + \left(\frac{a_{H^+}\, a_{Cl^-}}{K_{HCl}}\right)$$

can be solved for a_{H^+}. Having determined a_{K^+} and a_{H^+}, the ratio a_{K^+}/a_{H^+} can be calculated for each point on the reaction boundary. Inspection of Table 2 in Shade (1974) shows that these calculations do not make use of the assumption Σ K = Σ Cl (as stated); whereas Σ K always is 2, Σ Cl ranges as high as 3.

Values of log (a_{K^+}/a_{H^+}) from Shade (1974) are listed in Table 5 and from these it is possible to calculate -RT ln (a_{K^+}/a_{H^+}). Plotting this function, at 500°C and 600°C, against (P-1) an approximately straight line is obtained (Fig. 13) suggesting a constant volume of reaction since

$$-RT \ln K = \Delta G^\circ + \Delta V\,(P-1)$$

ΔG° of the reaction at 1 bar (practically the same as at 1 atm) is obtained from the intercept at (P-1) = 0. The slope gives ΔV, and subtracting $\Delta V_{solids} = -0.5949$ calories/bar (Chatterjee and Johannes, 1974), one obtains $(\bar{V}^\infty_{K^+} - \bar{V}^\infty_{H^+})$. These volume differences along with values at low temperatures taken from Ellis and McFadden (1972), are plotted in Figure 14. It is obvious that the volume difference varies markedly with temperature.

From Figure 13 it is seen that $\Delta G°$ at 600°C is -9680 calories. Thermochemical calculations based on data in Robie et al. (1978) give a value of -10 049 calories at 25°C. Also $\Delta S°$ at 25°C is 7.01 calories/°K. Assuming a constant ΔC_P° of reaction

$$\Delta S^\circ_{298.15} = \Delta S_I + \Delta a \ln (298.15)$$

and

$$\Delta S_I = \Delta S^\circ_{298.15} - \Delta a \ln (298.15)$$

can be substituted in the equation

$$\Delta G° = \Delta H_I - T(\Delta S_I - \Delta a) - \Delta a T \ln T$$

This equation can be solved for ΔH_I and Δa if $\Delta G°$ is known at two temperatures. Accepting the values at 600° and 25°C the following relationship is obtained:

$$\Delta G° = -4347 - 88.145\ T + 12.114\ T \ln T$$

which is plotted in Figure 15.

Table 5. The hydrolysis of K feldspar

$$1.5\ KAlSi_3O_8 + H^+ \leftrightharpoons 0.5\ KAl_2Si_3AlO_{10}(OH)_2 + 3\ SiO_2 + K^+$$

T (°C)	P (kilobars)	$\log \left(\frac{a_{K^+}}{a_{H^+}}\right)$	$-RT \ln \left(\frac{a_{K^+}}{a_{H^+}}\right)$	ΔG° (calories)
Shade (1974)				
400	1	3.940	-12 136	-11 571
400	2	4.146	-12 770	-11 639
400	3	4.169	-12 841	-11 144
400	4	4.487	-13 820	-11 557
500	1	3.529	-12 484	-11 812
500	2	3.305	-11 692	-10 348
500	3	3.346	-11 837	- 9 821
500	4	3.662	-12 955	-10 267
500	5	3.858	-13 648	-10 288
500	6	3.981	-14 083	-10 050
500	7	4.215	-14 911	-10 206
600	1	2.645	-10 567	- 9 762
600	2	2.911	-11 630	-10 020
600	3	2.922	-11 674	- 9 259
600	4	3.162	-12 633	- 9 412
600	5	3.445	-13 763	- 9 737
600	6	3.679	-14 698	- 9 866
600	7	3.840	-15 342	- 9 705
625	1	1.697	- 6 974	- 6 128
645	1	1.448	- 6 083	- 5 201
650	3	2.778	-11 734	- 9 059
670	2	2.387	-10 301	- 8 438
Montoya and Hemley (1975)				
300	1	4.075	-10 687	-10 210
400	1	3.557	-10 956	-10 391
500	1	3.231	-11 430	-10 758
600	1	2.292	- 9 157	- 8 352
Usdowski and Barnes (1972)				
30	0.001	6.01	- 8 336	- 8 336
60	0.001	5.86	- 8 933	- 8 933
300	0.085	4.22	-11 067	-11 027
Thermochemical calculation				
25	1 atm	—	—	-10 049

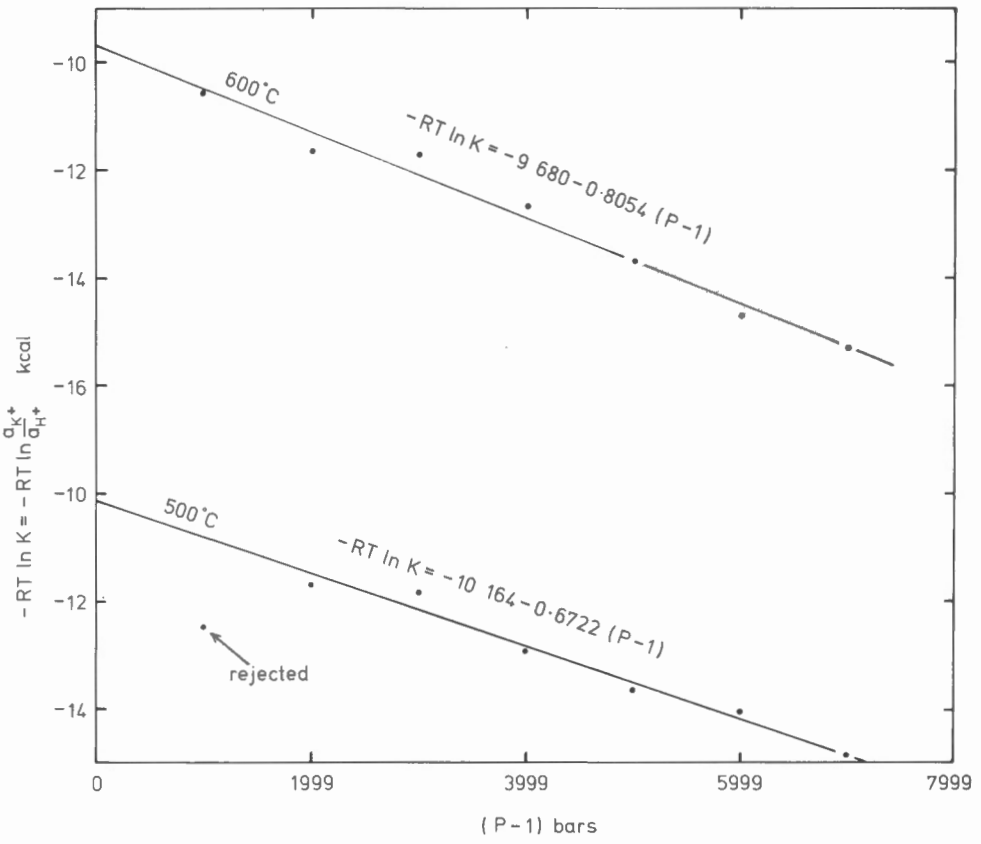

Figure 13. *The variation with pressure of -RT ln K for the hydrolysis of K feldspar.*

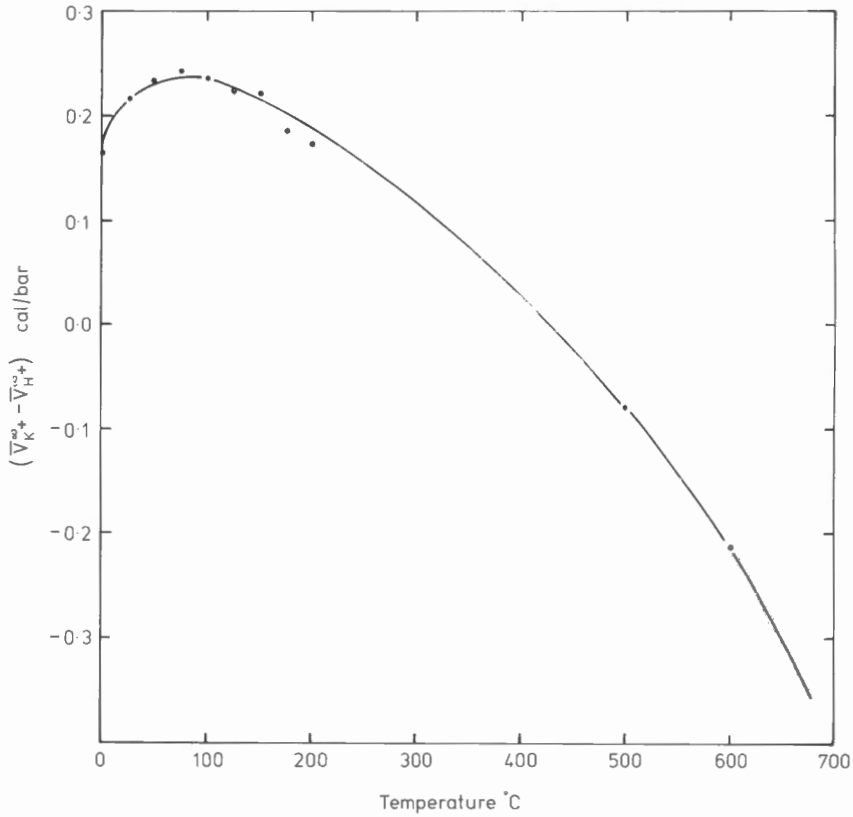

Figure 14. *The variation of the molar volume change ($\overline{V}^{\infty}_{K^+} - \overline{V}^{\infty}_{H^+}$) with temperature.*

The equilibrium constant of the hydrolysis of K feldspar at lower temperatures has been determined by Usdowski and Barnes (1972). Calculated values of $\Delta G°$ are plotted in Figure 15 where a considerable scatter of points is evident. At low temperatures, some discrepancy could be due to the structural state of feldspar. Shade (1974) and Usdowski and Barnes (1972) used adularia as a starting material. It is likely that adularia inverted to sanidine in the experiments at 500° and 600°C whereas in the low-temperature experiments the feldspar would have a different structural state. At 300°C, log K = 4.11 and assuming $a_{K^+} = 0.5$ m, pH = 4.41. The resultant muscovite-K feldspar boundary is plotted in Figure 16.

The Stability of Biotite

In spite of a considerable amount of experimental work, the free energy of formation of the end member annite is not well known. To a large extent this is due to the difficulty of determining the content of ferric iron in synthetic biotites. It is a common observation that biotites coexisting with pyrite are relatively Mg-rich, even at the triple point pyrite-pyrrhotite-magnetite. For example, Beane (1974) reported an annite content of about 35 per cent in biotite coexisting with these three minerals. Assuming ideal mixing in the octahedral position and neglecting the mixing in the tetrahedral positions there is the relation that

$$a_{KFe_3Si_3AlO_{10}(OH)_2} = X^3_{KFe_3Si_3AlO_{10}(OH)_2} = \left(\frac{Fe}{Fe+Mg}\right)^3$$

For the oxidation of annite

$$KFe_3Si_3AlO_{10}(OH)_2 + \tfrac{1}{2}O_2 \leftrightharpoons KAlSi_3O_8 + H_2O + Fe_3O_4$$

the equilibrium constant is given by

$$\log K = \log a_{H_2O} - \tfrac{1}{2}\log f_{O_2} - \log a_{KFe_3Si_3AlO_{10}(OH)_2}$$

or

$$\log K - \log a_{H_2O} = -\tfrac{1}{2}\log f_{O_2} - \log a_{KFe_3Si_3AlO_{10}(OH)_2}$$

For a given f_{O_2} ($\log f_{O_2} = -33.48$ at the triple point) and activity of annite (at the triple point, Fe/(Fe+Mg) = 0.35), $\log K - \log f_{H_2O}$ can be determined. Knowing this value it is possible to solve for $\log f_{O_2}$ at any chosen composition. Thus

Fe/(Fe+Mg)	$\log f_{O_2}$
0.15	-31.27
0.35	-33.48
0.55	-34.66

These composition contours can be plotted in the magnetite field; K feldspar is also stable. Some of the contours intersect the pyrrhotite-magnetite boundary, giving rise to the reaction

$$KFe_3Si_3AlO_{10}(OH)_2 + 3H^+ + HS^- \leftrightharpoons KAlSi_3O_8 + 3FeS + 4H_2O$$

which is independent of $\log f_{O_2}$. The 0.15 contour intersects the pyrite-magnetite boundary. Its continuation can be plotted according to slopes on a $\log f_{O_2}$-pH diagram obtained from reactions:

$$KFe_3Si_3AlO_{10}(OH)_2 + 12H^+ + 6SO_4^= \leftrightharpoons KAlSi_3O_8 + 3FeS_2 + 7H_2O + \frac{21}{2}O_2$$

slope = -24:21

$$KFe_3Si_3AlO_{10}(OH)_2 + 6H^+ + 6HS^- + \frac{3}{2}O_2 \leftrightharpoons KAlSi_3O_8 + 3FeS_2 + 7H_2O$$

slope = 4:1

Comments

According to the developed $\log f_{O_2}$-pH diagram (Fig. 16), biotite is restricted to an alkaline and reducing environment (except very Mg-rich biotite). Biotite would not be expected to occur with muscovite. This inference is consistent with the view expressed by Jambor and Beaulne (1978) that sericite found in biotite-K feldspar rocks is part of a later assemblage overprinted on an early potassic alteration. Chalcopyrite becomes insoluble in the potassic zone (biotite and K feldspar); it is soluble in the phyllic zone, accounting for its typical absence in this zone.

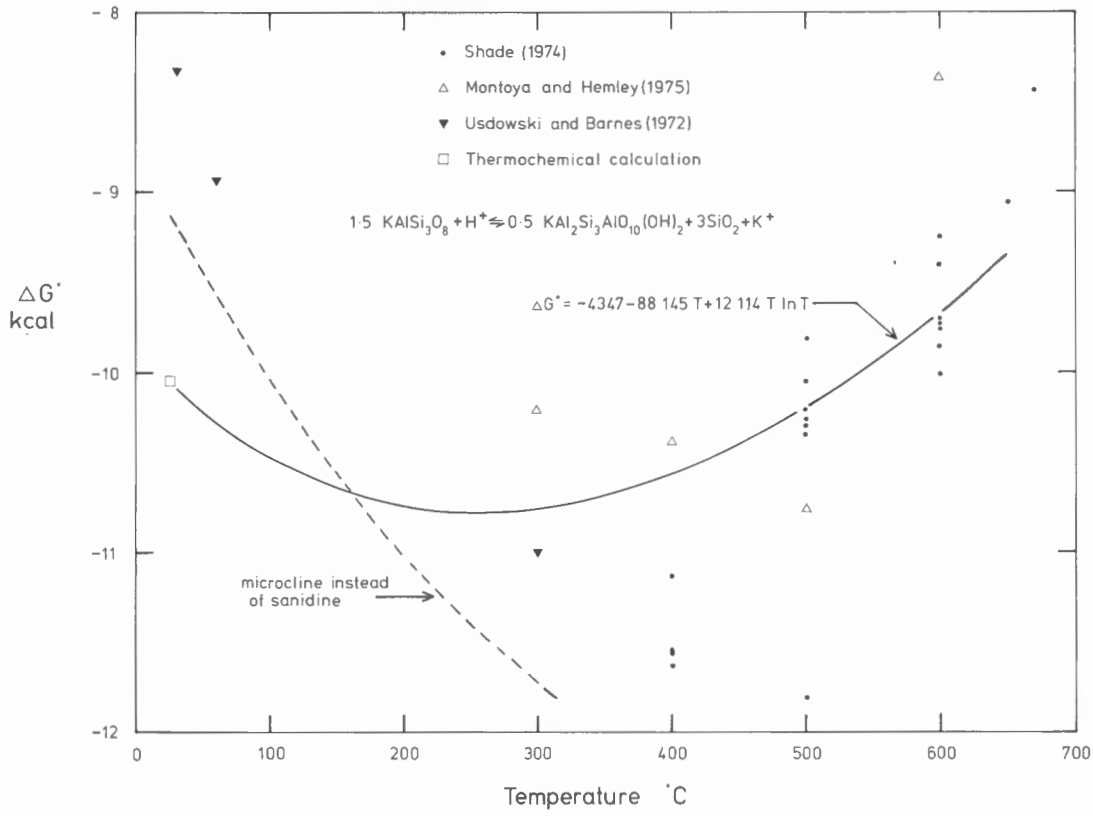

Figure 15. *The variation with temperature of the standard Gibbs free energy change (ΔG^0) for the hydrolysis of K feldspar.*

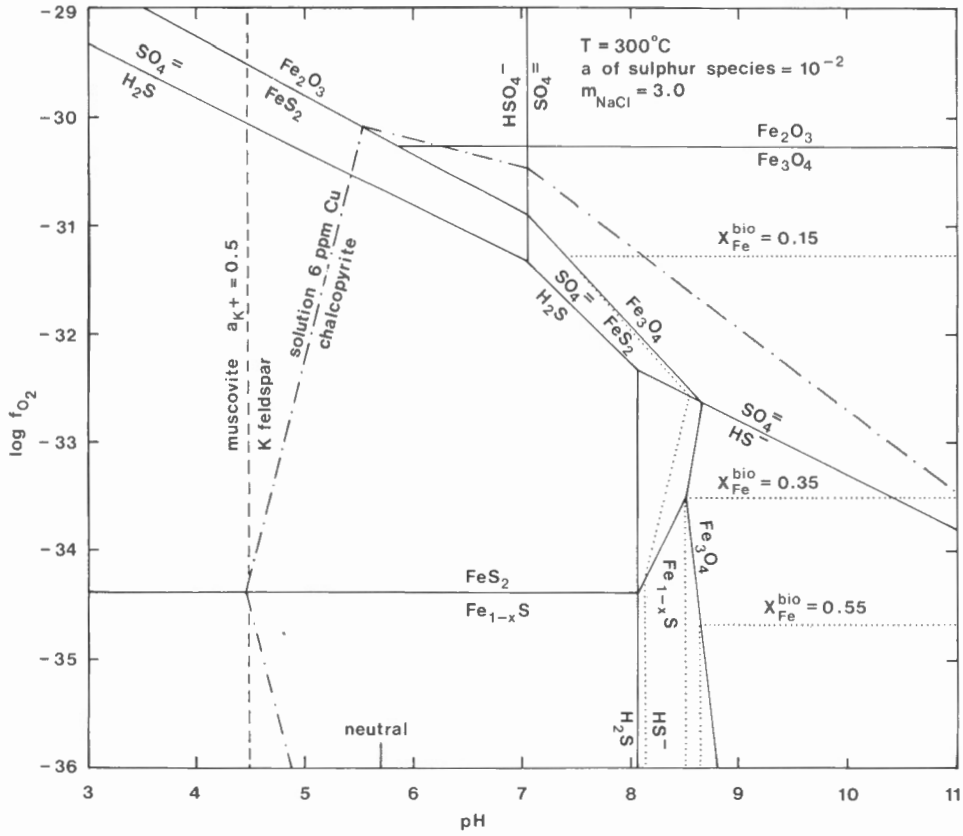

Figure 16. *Mineral stabilities in porphyry copper deposits.*

METAMORPHISM OF SULPHIDE DEPOSITS

During metamorphism sulphides may equilibrate among themselves and with coexisting oxides and silicates. If compatible mineral assemblages can be determined, sulphide-silicate-oxide equilibria give some indication of metamorphic conditions. Quenching of sulphide-bearing assemblages appears difficult. Nevertheless, regularities in mineral assemblages suggest that some mineralogical features established during metamorphism are preserved. The following observations will be discussed in terms of phase equilibria, noting attendant problems of quenching:

1. In some rocks, a high modal amount of sulphides is correlated with iron-poor silicates and commonly pyrite coexists with iron-poor silicates and pyrrhotite with iron-rich silicates.
2. In a few occurrences, gahnite ($ZnAl_2O_4$) preferentially occurs in iron-rich rocks with low modal amounts of sulphides.
3. There is a correlation of the compositions of coexisting sphalerite and pyrrhotite.

The System Fe-S

The composition of pyrrhotite is commonly expressed by one of two mole fraction scales that are related to the atomic fraction Fe/(Fe+S) as follows:

$$N_{FeS} = \left(\frac{FeS}{FeS + S_2}\right) = 2\left(\frac{Fe}{Fe + S}\right); \; X_{FeS} = \left(\frac{FeS}{FeS + S}\right) = \left(\frac{Fe}{S}\right)$$

The composition of hexagonal pyrrhotite (stable above 325°C) coexisting with pyrite is well-known. There is a good agreement among the results of Arnold (1962), Toulmin and Barton (1964), and Schneeberg (1973). The pyrite-pyrrhotite curve is terminated at 743°C where it intersects the sulphur condensation curve.

Toulmin and Barton (1964) measured log f_{S_2} of the vapour coexisting with pyrrhotite as a function of N_{FeS} and T and derived an empirical relationship (their equation (8)). More recent work by Rau (1976) and Fryt et al. (1979) gave comparable results. The activity of FeS in pyrrhotite was determined by integrating the Gibbs-Duhem equation

$$N_{FeS} \; d \log a_{FeS} = -N_{S_2} \; d \log f_{S_2}$$

It is stated in many texts (e.g. Glasstone, 1947; Darken and Gurry, 1953) that it is imprecise to integrate the Gibbs-Duhem equation in terms of activities, because the logarithm of the activity of a component $\to -\infty$ as $X \to 0$. This is true only if the component in question cannot have negative values. If FeS is chosen as a component, S_2 has a finite activity as $N_{FeS} \to 1$ and there is no difficulty in integrating the equation (Froese and Gunter, 1978). The equation can be integrated by plotting $(N_{FeS}-1)/N_{FeS}$ against log f_{S_2} and determining the area under the curve. This can be done analytically by expressing $(N_{FeS}-1)/N_{FeS}$ as a power series in log f_{S_2}. However, Toulmin and Barton (1964) chose a different method. Differentiation of their equation (8) provided an expression of d log f_{S_2} as a function of N_{FeS} and T and, by integration, they obtained log a_{FeS} as a function of N_{FeS} and T (their equation (13)).

More recently, Schneeberg (1973) determined the pyrite-pyrrhotite equilibrium. Although the composition of pyrrhotite agrees very well with values reported by Toulmin and Barton (1964), log f_{S_2} differs by about 0.3. This leaves three options:

1. Accept Schneeberg's f_{S_2} values, reject equations (8) and (11) of Toulmin and Barton (1964), and proceed with a new integration of the Gibbs-Duhem equation.
2. Reject Schneeberg's f_{S_2} values. This has been done here, mainly in order to retain equations (8) and (11) of Toulmin and Barton (1964).
3. Accept Schneeberg's f_{S_2} values and equations (8) and (11) of Toulmin and Barton (1964). This requires a shift in the composition of pyrrhotite (Fig. 17), again not a satisfactory procedure.

It should be realized that the simultaneous acceptance of the experimental pyrrite-pyrrhotite solvus, of equations (8) and (11) of Toulmin and Barton (1964), and of Schneeberg's (1973) f_{S_2} values, as was done by Craig and Scott (1974), is not consistent.

The Stability of Fe-Mg Amphibole

The stability of iron-magnesium silicates is conveniently shown as a set of contours on a log f_{O_2}-log f_{S_2} diagram (Froese, 1971). First, such a diagram at 2 kilobars and 700°C (Fig. 18) is constructed, using thermodynamic properties given in Table 6. To calculate f_{S_2} for a given pyrrhotite composition, an approach suggested by LeCheminant (1973) is used. The following equilibrium is valid between sulphur vapour and the component □S inpyrrhotite, were □ stands for a vacancy:

$$\square S \text{ (in pyrrhotite)} \leftrightharpoons \tfrac{1}{2} S_2 \text{ (in vapour)}$$

$$\Delta G^\circ = -\tfrac{1}{2} RT \ln f_{S_2} + RT \ln a_{\square S} - \Delta V_s (P-1)$$

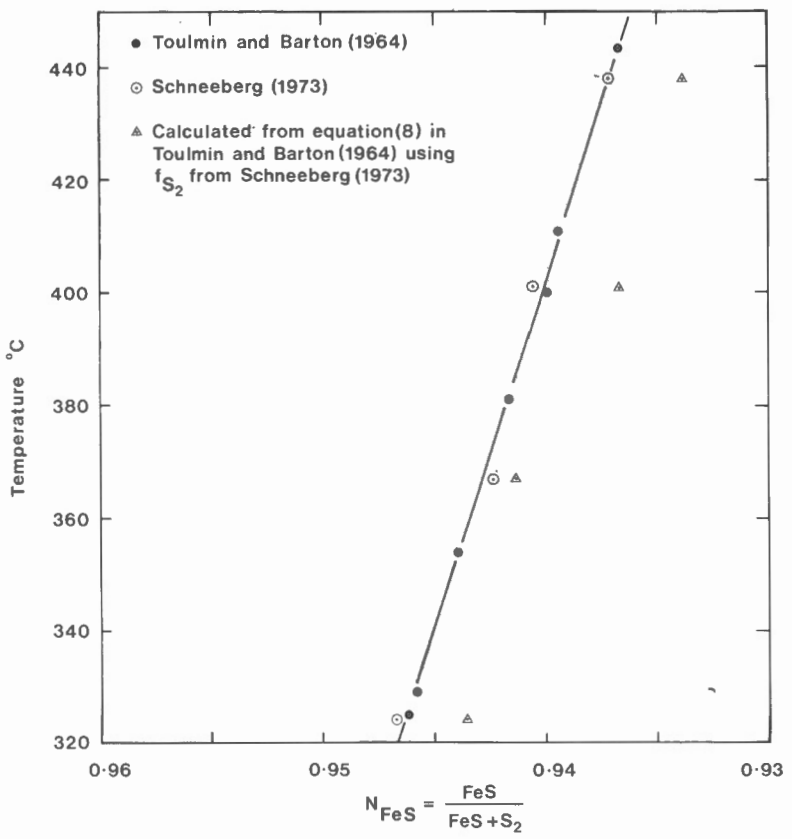

Figure 17. *The composition of pyrrhotite coexisting with pyrite.*

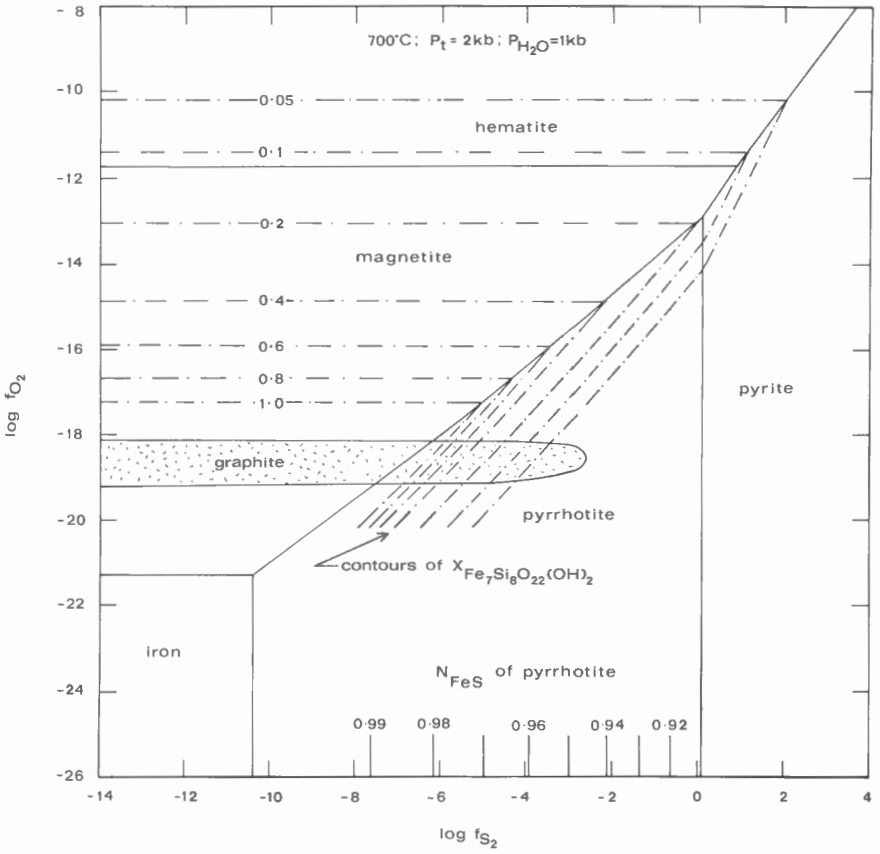

Figure 18. *The oxidation and sulphidation of Fe-Mg amphibole (modified from Froese, 1977).*

The molar volume of pyrrhotite solid solution (FeS- S), plotted against X_{FeS}, is approximately linear (Froese and Gunter, 1976). Therefore, for a given composition, the activities of both components are constant and independent of pressure. Since f_{S_2} is known at one atmosphere (Toulmin and Barton, 1964) it is possible to calculate $\Delta G^\circ - RT \ln a_S$ and, therefore, f_{S_2} at any pressure can be found.

The composition of pyrrhotite coexisting with either iron or pyrite at 2 kilobars (Table 7) has to be found by trial and error. A given pyrrhotite composition provides values of f_{S_2} and a_{FeS} and these values must satisfy the equilibrium constant equation

$$\Delta G^\circ = -RT \ln K - \Delta V_s (P-1)$$

for reactions (1) and (3) in Table 6. Knowing f_{S_2} and a_{FeS} for a given pyrrhotite composition, the corresponding f_{O_2} along the magnetite-pyrrhotite boundary can be calculated from reaction (5) in Table 6. Results are listed in Table 7; very slight differences will be noted between Table 7 and Table 6.1 in Froese (1977) because a solution model for pyrrhotite was used which is valid above 600°C. The advantage of the present method is that it can be used at any temperature.

The triple point hematite-magnetite-pyrite is obtained from the intersection of reaction (6) in Table 6 with the reaction

$$Fe_3O_4 + 3S_2 \leftrightharpoons 3FeS_2 + 2O_2$$

The slope of this reaction as well as that of the reaction

$$Fe_2O_3 + 2S_2 \leftrightharpoons 2FeS_2 + \tfrac{3}{2} O_2$$

is obtained from the reaction equation.

From the experimental work of Popp et al. (1977), Froese (1977) derived free energy changes of oxidation and sulphidation reactions involving Fe-Mg amphibole and plotted composition contours on a log f_{O_2}-log f_{S_2} diagram. It is also possible to show the stability of graphite on this diagram. As pointed by Miyashiro (1964), graphite is restricted to low values of f_{O_2}. But graphite becomes unstable not only when P_{CO_2} exceeds 1 kilobar but also when the sum of the partial pressures of gas species other than H_2O exceeds 1 kilobar. Figure 18 was calculated for P_{H_2O} = 1 kilobar. The stability field of graphite can be outlined by carrying out calculations described by Eugster and Skippen (1967). It is apparent that at the conditions represented in Figure 18, graphite and pyrite do not stably coexist.

Table 6. Thermodynamic properties at 700°C and 2 kilobars

Reaction	ΔG° calories	$\Delta V_s(P-1)$ calories	Reference for ΔG°
(1) $Fe + \frac{1}{2}S_2 \leftrightharpoons FeS$	-23 666	531	Toulmin and Barton (1964)
(2) $\square S$ (in pyrrhotite) $\leftrightharpoons \frac{1}{2}S_2$ (in vapour)		-691	
(3) $FeS + \frac{1}{2}S_2 \leftrightharpoons FeS_2$	-1 759	274	Toulmin and Barton (1964)
(4) $3Fe + 2O_2 \leftrightharpoons Fe_3O_4$	-190 951	1111	Haas and Robie (1973)
(5) $Fe_3O_4 + \frac{3}{2} S_2 \leftrightharpoons 3FeS + 2O_2$	+119 953	481	
(6) $2Fe_3O_4 + \frac{1}{2}O_2 \leftrightharpoons 3Fe_2O_3$	-26 089	85	Haas and Robie (1973)

Note: For reactions (1) and (3), ΔG° has been calculated from known values of f_{S_2} and a_{FeS} at one atmosphere. The molar volumes of solids have been taken from Robie et al. (1978) with the exception of the molar volume of $\square S$ which has been taken from Froese and Gunter (1976).

Table 7. The pyrrhotite-magnetite equilibrium at 700°C

N_{FeS}	X_{FeS}	a_{FeS}	log f_{S_2}		log f_{O_2}	
			1 atmosphere	2 kilobars	1 atmosphere	2 kilobars
1.0001	1.0002	1.000		10.37*		-21.30
1.0000	1.0000	1.000	-10.63*		-21.44	
0.9900	0.9802	0.974	-8.04	-7.73	-19.48	-19.30
0.9800	0.9608	0.923	-6.49	-6.18	-18.28	-18.10
0.9700	0.9417	0.858	-5.26	-4.95	-17.31	-17.13
0.9600	0.9231	0.786	-4.21	-3.90	-16.47	-16.29
0.9500	0.9048	0.711	-3.28	-2.97	-15.71	-15.53
0.9400	0.8868	0.634	-2.44	-2.13	-15.00	-14.82
0.9300	0.8692	0.560	-1.65	-1.34	-14.33	-14.15
0.9200	0.8519	0.488	-0.92	-0.61	-13.69	-13.51
0.9100	0.8349	0.421	-0.23	0.08**	-13.08	-12.90
0.9064	0.8288	0.398	0.01**		-12.86	

* Coexisting with iron
** Coexisting with pyrite

Phase relations in the presence of magnetite can be shown on a triangular composition diagram, if one component is chosen as $FeO - Fe_2O_3$ (projection through magnetite). Figure 19 demonstrates that a low sulphur content of a rock will give rise to pyrrhotite and a high content to pyrite. It also shows that pyrite is stable only with very Mg-rich silicates. This raises a considerable problem in interpreting natural assemblages, because pyrite is found in rocks sufficiently iron-rich to contain almandine and staurolite. One possible explanation could be that many rocks pass through the stability field of pyrite on cooling and part of the pyrrhotite is converted to pyrite.

The Stability of Gahnite

Zinc, like iron, enters into sulphide (sphalerite), oxide (gahnite), and silicate (staurolite). Therefore, gahnite plays an interesting, but as yet poorly understood, role in the metamorphism of ores. Observations of natural assemblages do not display easily recognizable regularities and a great deal of further petrographic documentation is required.

Some insight into this problem is gained from the reaction

$$ZnAl_2O_4 + \tfrac{1}{2}S_2 \leftrightharpoons ZnS + Al_2O_3 + \tfrac{1}{2}O_2$$

For a given activity of Al_2O_3, the slope on a log f_{O_2}-log f_{S_2} diagram is 1:1. Within the pyrrhotite field, this reaction separates iron-rich amphiboles coexisting with gahnite from iron-poor amphiboles coexisting with sphalerite (Fig. 18). Such a conclusion is also reached by projecting phase relations in the system FeO-MgO-ZnS-FeS through FeS (Fig. 20; see also Froese and Moore, 1980). In one example, described by Juve (1967) gahnite occurs in rocks with disseminated sulphides whereas sphalerite occurs in massive ore (Fig. 21). However, in this case no compositions are given. From another example, the Amulet mine in Quebec, the composition of anthophyllites coexisting with magnetite, chlorite, and cordierite is plotted (Kelly, 1975). The one recorded occurrence of gahnite comes from the most iron-rich rock (Fig. 22) although it is recognized that probably some differences in T and/or P_{H_2O} existed from rock to rock and that the presence of pyrite in iron-rich rocks might indicate re-equilibration at low temperatures.

For these reasons, there is some support for the indicated coexistence of gahnite with Fe-rich amphibole and sphalerite with Mg-rich amphibole in Figure 19. The boundary should fall within the pyrrhotite-amphibole stability field to account for the common coexistence of sphalerite and pyrrhotite. The point that separates amphiboles coexisting with pyrite from those coexisting with pyrrhotite can be extended as a boundary cutting across an AFM diagram (see Froese, 1976, p. 34). Similarly, there exists a gahnite-sphalerite boundary within the pyrrhotite field. Mineral assemblages shown in an AFM diagram also can be represented by a subdivision of the biotite composition surface into mineral stability fields (Froese, 1978). On such a biotite composition surface (Fig. 23) it is possible to show the pyrite-pyrrhotite boundary and the gahnite-sphalerite boundary (Froese and Moore, 1980).

The System FeS-ZnS-S

In the system Fe-S, the composition of pyrrhotite coexisting with pyrite is a function of pressure and temperature. The same is true of the composition of sphalerite, coexisting with pyrite and pyrrhotite, in the system Fe-S-Zn. The composition of pyrrhotite coexisting with pyrite at 700°C and 2 kilobars has been calculated already. Similar calculations can be carried out at other pressure and temperature combinations. The results can be shown as contours of pyrrhotite composition on a P-T diagram (Fig. 24). On this diagram contours of sphalerite composition, coexisting with pyrite and pyrrhotite, are also shown according to calculations by Hutcheon (1978, 1980). The calculations are in close agreement with experimental determinations by Scott (1973).

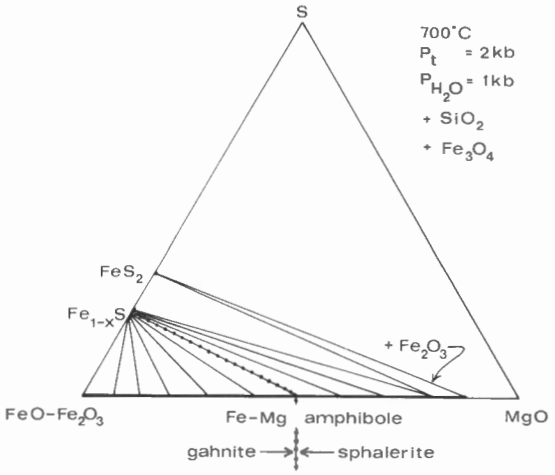

Figure 19. The composition of Fe-Mg amphibole coexisting with iron sulphides in the presence of magnetite (modified from Froese, 1977).

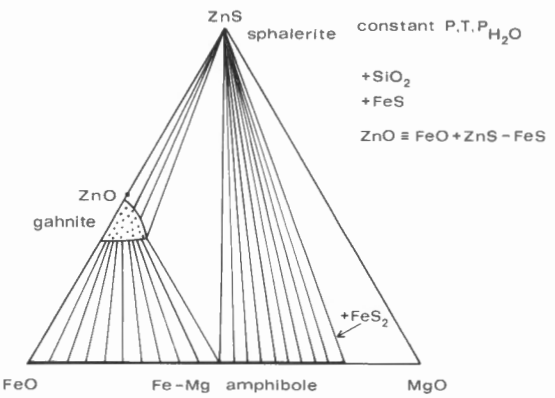

Figure 20. The composition of Fe-Mg amphibole coexisting with zinc minerals in the presence of pyrrhotite.

Hutcheon (1978) fitted a solution model to experimental data of Barton and Toulmin (1966). This, together with the molar volume of sphalerite solid solution, provides formulae that allow the calculation of γ_{FeS} in sphalerite at any temperature, pressure, and composition. Also for the equilibrium

$$FeS \text{ (in pyrrhotite)} \leftrightharpoons FeS \text{ (in sphalerite)}$$

the standard free energy change was found to be

$$\Delta G^\circ = 239 + 0.840\ T \text{ (not } 239 - 0.840\ T, \text{ as stated in Hutcheon, 1978)}$$

Knowing a_{FeS} in pyrrhotite on the pyrite-pyrrhotite solvus, it is possible, by trial and error, to find a sphalerite composition which satisfies the above equation. Thus the composition of sphalerite, coexisting with pyrite and pyrrhotite, is calculated at 1 atmosphere. In calculations at higher pressure (Hutcheon, 1980), it is necessary to consider thermal expansion and isothermal compression, as suggested by Scott (1973). As an example, the composition of sphalerite has been calculated at 400°C and 5 kilobars. The change in volume as calculated for troilite and sphalerite has been applied to the component □S and FeS (sphalerite), respectively. Thus the following volumes in cubic centimetres are obtained (the volumes at 25°C and 1 atmosphere, taken from Froese and Gunter (1976) and Hutcheon (1978), are given in brackets): FeS 18.871 (18.198), □S 15.131 (14.458), FeS_2 24.166 (23.940), FeS sphalerite 24.092 (24.033). Calculations are carried out using thermodynamic properties listed in Table 8.

By trial and error, the composition of pyrrhotite coexisting with pyrite at 500°C and 5 kilobars is found to be $N_{FeS} = 0.9475$ ($X_{FeS} = 0.9002$). For this composition $a^{po}_{FeS} = 0.608$ and $\log f_{S_2} = -7.06$; these values satisfy the second equation in Table 8. Also by trial and error, the composition of sphalerite is found to be $X_{FeS} = 0.138$ corresponding to $a^{sp}_{FeS} = 0.209$. The activities of FeS in pyrrhotite and sphalerite satisfy the third equation in Table 8.

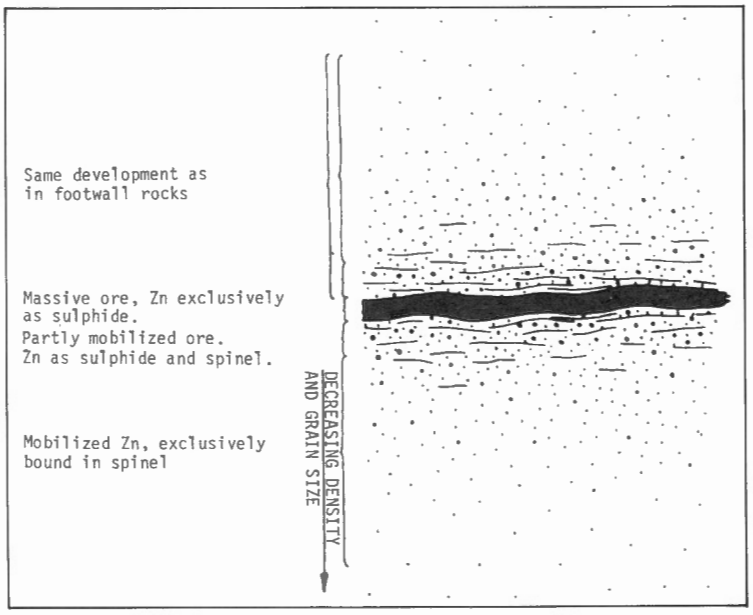

Figure 21

Typical distribution of gahnite and sphalerite in ore deposits of the Håfjell syncline, Ofoten fiord, northern Norway (from Juve, 1967; by permission of Universitetsforlaget Oslo-Bergen-Tromsø).

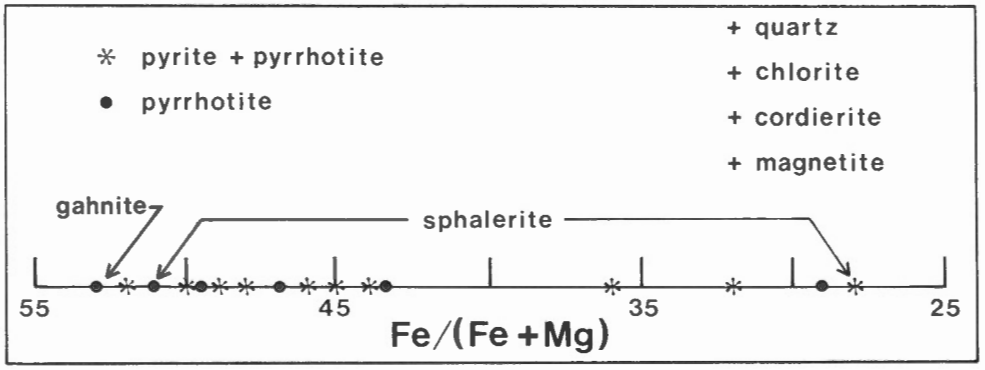

Figure 22. *The composition of anthophyllite coexisting with zinc minerals from the Amulet mine (from Kelly, 1975).*

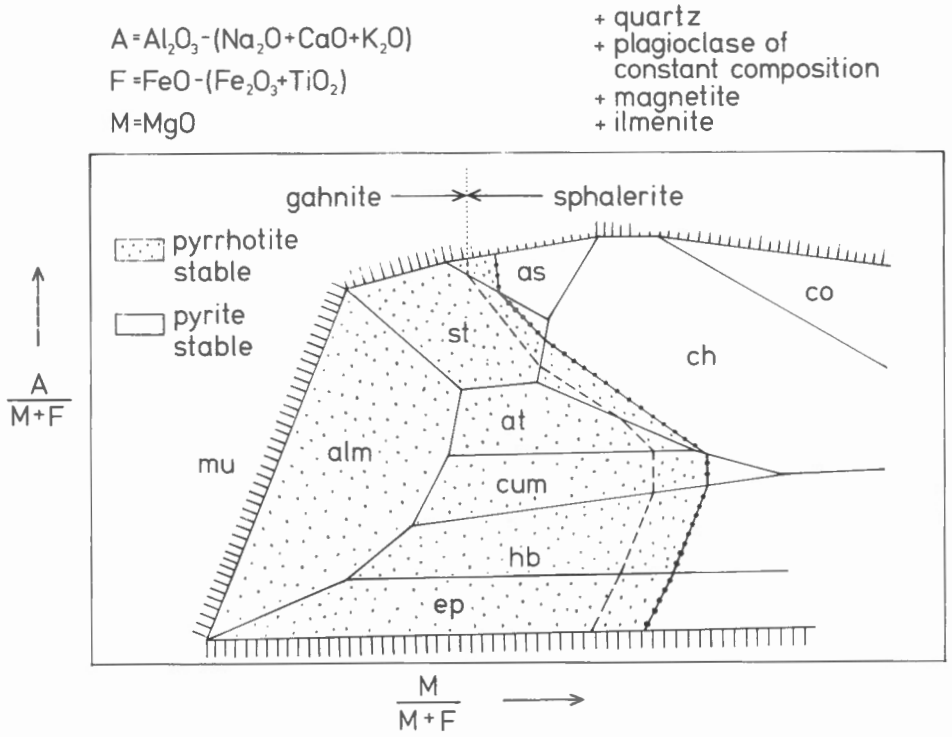

mu – *muscovite* *st* – *staurolite* *at* – *anthophyllite*
ch – *chlorite* *alm* – *almandine* *cum* – *cummingtonite*
as – *alluminum silicate* *co* – *cordierite* *hb* – *hornblende*
ep – *epidote*

Figure 23. *Mineral assemblages from the Snow Lake area, Manitoba, shown on the biotite composition surface (from Froese and Moore, 1980).*

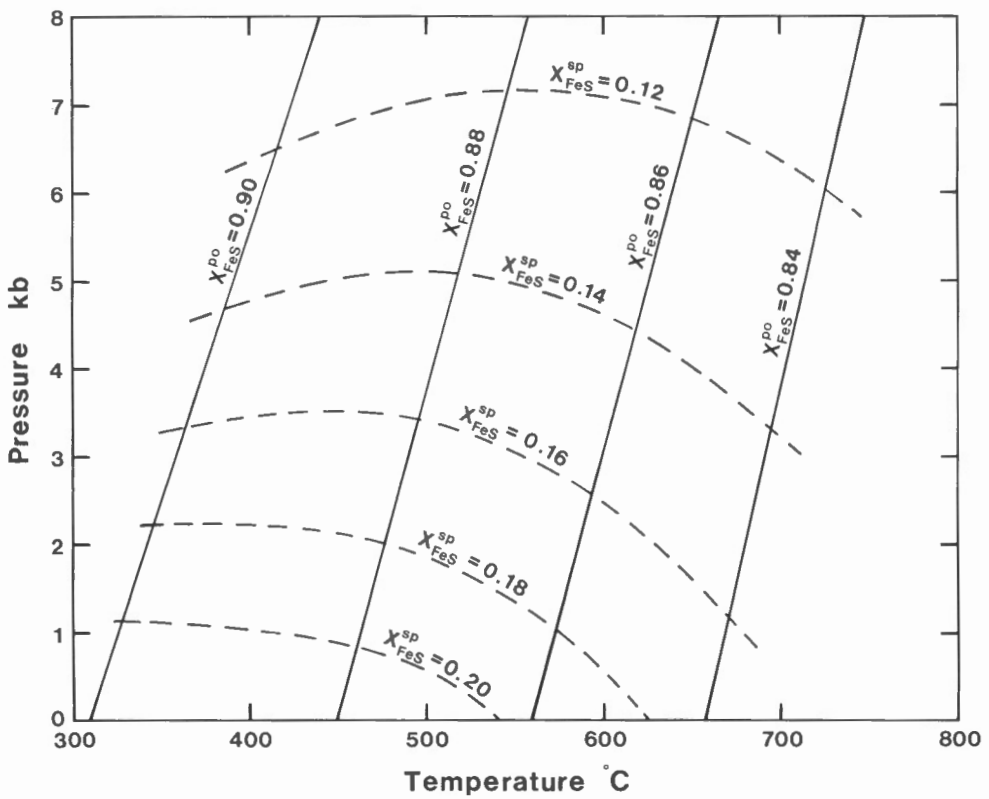

Figure 24. *The composition of pyrrhotite (po) and sphalerite (sp) from the assemblage pyrite-pyrrhotite-sphalerite.*

Table 8. Thermodynamic Properties at 400°C and 5 kilobars

Reaction	ΔG^0 calories	$\Delta V_S(P-1)$ calories	Reference for ΔG^0
□S (in pyrrhotite)⇋½S_2 (in vapour)		-1808	
FeS + ½S_2⇋FeS_2	-12 174	633	Toulmin and Barton (1964)
FeS (in pyrrhotite)⇋FeS (in sphalerite)	804	624	Hutcheon (1978)

Note: At one atmosphere the composition of pyrrhotite coexisting with pyrite has been taken as 0.9405 from a fit to the points given in Table 5 of Toulmin and Barton (1964). For this composition $\log f_{S_2} = -7.37$ and $a_{FeS} = 0.540$; thus ΔG^0 of the second reaction can be calculated to be -12 174 calories.

Thus one measured tie line sphalerite-pyrrhotite in the presence of pyrite should give pressure and temperature (Fig. 24). But unfortunately, the composition of pyrrhotite does not quench easily. In view of the flat composition contours of sphalerite, its composition at an estimated temperature has been used as a geobarometer, following the work of Scott and Barnes (1971) and Scott (1973). But there is growing evidence that sphalerite also changes its composition during cooling. Thus Bristol (1979) found that in rocks with abundant monoclinic pyrrhotite (inverted from high-temperature hexagonal pyrrhotite) sphalerite appeared to be anomalously Fe-poor giving excessive pressure estimates.

REFERENCES

Adams, L.H.
1936: Activity and related thermodynamic quantities; their definition, and variation with temperature and pressure; Chemical Reviews, v. 19, p. 1-26.

Anderson, G.M.
1973: The hydrothermal transport and deposition of galena and sphalerite near 100°C; Economic Geology, v. 68, p. 480-492.

1975: Precipitation of Mississippi Valley-type ores; Economic Geology, v. 70, p. 937-942.

1977: Thermodynamics and sulfide solubility; Mineralogical Association of Canada; Short Course Handbook, v. 2, p. 136-150.

Arnold, R.G.
1962: Equilibrium relations between pyrrhotite and pyrite from 325° to 743°C; Economic Geology, v. 57, p. 72-90.

Barnes, H.L. and Kullerud, G.
1961: Equilibria in sulfur-containing aqueous solutions, in the system Fe-S-O, and their correlation during ore deposition; Economic Geology, v. 56, p. 648-688.

Barton, P.B. Jr. and Toulmin, P. III
1966: Phase relations involving sphalerite in the Fe-Zn-S system; Economic Geology, v. 61, p. 815-849.

Beane, R.E.
1974: Biotite stability in the porphyry copper environment; Economic Geology, v. 69, p. 241-256.

Biegler, T. and Woods, R.
1973: The standard hydrogen electrode; Journal of Chemical Education, v. 50, p. 604-605.

Bristol, C.C.
1979: Application of sphalerite geobarometry to ores from the Ruttan mine; Economic Geology, v. 74, p. 1496-1503.

Chatterjee, N.D. and Johannes, W.
1974: Thermal stability and standard thermodynamic properties of synthetic $2M_1$ – muscovite $KAl_2[AlSi_3O_{10}(OH)_2]$; Contributions to Mineralogy and Petrology, v. 48, p. 89-114.

Craig, J.R. and Scott, S.D.
1974: Sulfide phase equilibria; Mineralogical Society of America, Short Course Notes, v. 1, p. CS 1-CS 110.

Crerar, D.A. and Barnes, H.L.
1976: Ore solution chemistry V. Solubilities of chalcopyrite and chalcocite assemblages in hydrothermal solution at 200° to 350°C; Economic Geology, v. 71, p. 772-794.

Darken, L.S. and Gurry, R.W.
1953: Physical chemistry of metals; McGraw-Hill, New York.

Day, H.W. and Halbach, H.
1979: The stability field of anthophyllite: the effect of experimental uncertainty on possible phase diagram topologies; American Mineralogist, v. 64, p. 809-823.

De Donder, T.
1920: Leçons de thermodynamique et de chimie physique; Gauthier-Villars, Paris.

Denbigh, K.
1971: The principles of chemical equilibrium, 3rd edition; Cambridge University Press, Cambridge.

Ellis, A.J. and McFadden, I.M.
1972: Partial molal volumes of ions in hydrothermal solutions; Geochimica et Cosmochimica Acta, v. 36, p. 413-426.

Eugster, H.P. and Skippen, G.B.
1967: Igneous and metamorphic reactions involving gas equilibria; in Researches in geochemistry, ed. P.H. Abelson, John Wiley, New York, v. 2, p. 492-520.

Everdell, M.H.
1965: Introduction to chemical thermodynamics; Norton and Company, New York.

Froese, E.
1969: Metamorphic rocks from the Coronation mine and surrounding area; Geological Survey of Canada, Paper 68-5, p. 55-77.

1971: The graphical representation of sulfide-silicate phase equilibria; Economic Geology, v. 66, p. 335-341.

1976: Applications of thermodynamics in metamorphic petrology; Geological Survey of Canada, Paper 75-43.

1977: Oxidation and sulphidation reactions; Mineralogical Association of Canada, Short Course Handbook, v. 2, p. 84-98.

1978: The graphical representation of mineral assemblages in biotite-bearing granulites; in Current Research, Part A, Geological Survey of Canada, Paper 78-1A, p. 323-325.

Froese, E. and Gunter, A.E.
1976: A note on the pyrrhotite-sulfur vapor equilibrium; Economic Geology, v. 71, p. 1589-1994.

1978: A note on the pyrrhotite-sulfur vapor equilibrium – a discussion; Economic Geology, v. 73, p. 286.

Froese, E. and Moore, J.M.
1980: Metamorphism in the Snow Lake area, Manitoba; Geological Survey of Canada, Paper 78-27.

Fryt, E.M., Smeltzer, W.W., and Kirkaldy, J.S.
1979: Chemical diffusion and point defect properties of iron sulfide (Fe_1-δS) at temperatures 600°-1000°C; Journal of the Electrochemical Society, v. 126, p. 673-683.

Garrels, R.M. and Christ, C.L.
1965: Solutions, minerals and equilibria; Harper and Row, New York.

Gibbs, J.W.
1876: On the equilibrium of heterogeneous substances; Transactions of the Connecticut Academy, v. 3, p. 108-248.

Glasstone, S.
1947: Thermodynamics for chemists; D. Van Nostrand Company, Princeton, New Jersey.

Haas, J.L., Jr. and Robie, R.A.
1973: Thermodynamic data for wüstite, $Fe_{0.947}O$, magnetite, Fe_3O_4, and hematite, Fe_2O_3 (abstract); Transactions of the American Geophysical Union, v. 54, p. 483.

Helgeson, H.C.
1969: Thermodynamics of hydrothermal systems at elevated temperatures and pressures; American Journal of Science, v. 267, p. 729-804.

Hemley, J.J.
1959: Some mineralogical equilibria in the system K_2O-Al_2O_3-SiO_2-H_2O; American Journal of Science, v. 257, p. 241-270.

Hutcheon, I.
1978: Calculation of metamorphic pressure using the sphalerite-pyrrhotite-pyrite equilibrium; American Mineralogist, v. 63, p. 87-95.

Hutcheon, I. (cont.)
1980: Calculated phase relations for pyrite-pyrrhotite-sphalerite: correction; American Mineralogist, v. 65, p. 1063-1064.

Jackson, S.A. and Beales, F.W.
1967: An aspect of sedimentary basin evolution: The concentration of Mississippi Valley-type ores during late stages of diagenesis; Bulletin of Canadian Petroleum Geology, v. 15, p. 383-433.

Jambor, J.L. and Beaulne, J.M.
1978: Sulphide zones and hydrothermal biotite alteration in porphyry copper-molybdenum deposits, Highland Valley, British Columbia; Geological Survey of Canada, Paper 77-12.

Juve, G.
1967: Zinc and lead deposits in the Håfjell syncline, Ofoten, northern Norway; Norges Geologiske Undersøkelse, no. 244.

Kelly, J.M.
1975: Geology, wall rock alteration and contact metamorphism associated with massive sulfide mineralization at the Amulet mine, Noranda district, Quebec; Ph.D. thesis, University of Wisconsin, Madison.

LeCheminant, A.N.
1973: Experimental control of H-O-S gas mixtures with applications to Fe-Ni sulfide-oxide-silicate reactions; Ph.D. thesis, University of British Columbia, Vancouver.

Large, R.R.
1977: Chemical evolution and zonation of massive sulfide deposits in volcanic terrains; Economic Geology, v. 72, p. 549-572.

Lewis, G.N. and Randall, M.
1961: Thermodynamics, 2nd edition; McGraw-Hill, New York.

Lowell, J.D. and Guilbert, J.M.
1970: Lateral and vertical alteration-mineralization zoning in porphyry ore deposits; Economic Geology, v. 65, p. 373-408.

Maier, C.G. and Kelley, K.K.
1932: An equation for the representation of high-temperature heat content data; Journal of the American Chemical Society, v. 54, p. 3243-3246.

Miyashiro, A.
1964: Oxidation and reduction in the earth's crust with special reference to the role of graphite; Geochimica et Cosmochimica Acta, v. 28, p. 717-729.

Montoya, J.W. and Hemley, J.J.
1975: Activity relations and stabilities in alkali feldspar and mica alteration reactions; Economic Geology, v. 70, p. 577-583.

Nriagu, J.O. and Anderson, G.M.
1971: Stability of the lead (II) chloride complexes at elevated temperatures; Chemical Geology, v. 7, p. 171-183.

Popp, R.K., Gilbert, M.C., and Craig, J.R.
1977: Stability of Fe-Mg amphiboles with respect to sulfur fugacity; American Mineralogist, v. 62, p. 13-30.

Rau, H.
1976: Energetics of defect formation and interaction in pyrrhotite $Fe_{1-x}S$ and its homogeneity range; Journal of Physical Chemistry of Solids, v. 37, p. 425-429.

Rentzsch, J.
1974: The *Kupferschiefer* in comparison with the deposits of the Zambian Copperbelt; in Gisements stratiformes et provinces cuprifères, ed. P. Bartholomé, Société Géologique de Belgique, Liège, p. 395-418.

Robie, R.A., Hemingway, B.S., and Fisher, J.R.
1978: Thermodynamic properties of minerals and related substances at 298.15 K and 1 bar (10^5 Pascals) pressure and at higher temperatures; United States Geological Survey, Bulletin 1452.

Roedder, E.
1967: Environment of deposition of stratiform (Mississippi Valley-type) ore deposits, from studies of fluid inclusions, in Genesis of stratiform lead-zinc-barite-fluorite deposits in carbonate rocks; ed. J.S. Brown, Economic Geology Monograph 3, p. 326-332.

Roscoe, S.M.
1965: Geochemical and isotopic studies, Noranda and Matagami areas; Canadian Institute of Mining and Metallurgy, Transactions, v. 68, p. 279-285.

Sato, M.
1971: Electrochemical measurements and control of oxygen fugacity and other gaseous fugacities with solid electrolyte systems; in Research techniques for high pressure and high temperature, ed. G.C. Ulmer, Springer-Verlag, New York, p. 43-99.

Schneeberg, E.P.
1973: Sulfur fugacity measurements with the electrochemical cell $Ag|AgI|Ag_{2+x}S, f_{S_2}$; Economic Geology, v. 68, p. 507-517.

Schottky, W., Ulich, H., and Wagner, C.
1929: Thermodynamik; Springer-Verlag, Berlin.

Scott, S.D.
1973: Experimental calibration of the sphalerite geobarometer; Economic Geology, v. 68, p. 466-474.

Scott, S.D. and Barnes, H.L.
1971: Sphalerite geothermometry and geobarometry; Economic Geology, v. 66, p. 653-669.

Shade, J.W.
1968: Hydrolysis equilibria in the system K_2O-Al_2O_3-SiO_2-H_2O; Ph.D. thesis, Pennsylvania State University, University Park.

1974: Hydrolysis reactions in the SiO_2-excess portion of the system K_2O-Al_2O_3-SiO_2-H_2O in chloride fluids at magmatic conditions; Economic Geology, v. 69, p. 218-228.

Sillén, L.G.
1959: Graphic presentation of equilibrium data; in Treatise on Analytical Chemistry, Part I, ed. I.M. Kolthoff and P.J. Elving; The International Encyclopedia, Inc., New York, v. 1, p. 277-317.

Spencer, J.N.
1974: ΔG and $\partial G/\partial \xi$; Journal of Chemical Education, v. 51, p. 577-579.

Toulmin, P. III and Barton, P.B. Jr.
1964: A thermodynamic study of pyrite and pyrrhotite; Geochimica et Cosmochimica Acta, v. 28, p. 641-671.

Truesdell, A.H.
1968: The advantage of using pE rather than Eh in redox equilibrium calculations; Journal of Geological Education, v. 16, p. 17-20.

Tunell, G.
1931: The definition and evaluation of the fugacity of an element or compound in the gaseous state; Journal of Physical Chemistry, v. 35, p. 2885-2913.

Usdowski, H.E. and Barnes, H.L.
1972: Untersuchungen über das Gleichgewicht zwischen K-Feldspat, Quarz and Muskovit und die Anwendung auf Fragen der Gesteinsbildung bei tieferen Temperaturen; Contributions to Mineralogy and Petrology, v. 36, p. 207-219.

Wedepohl, K.H.
1971: "Kupferschiefer" as a prototype of syngenetic sedimentary ore deposits; in Proceedings of IMA-IAGOD Meetings '70, IAGOD volume, ed. Y. Takéuchi, Society of Mining Geologists of Japan, Special Issue, no. 3, p. 268-273.

Whitmore, D.R.E.
1969: Geology of the Coronation copper deposit; Geological Survey of Canada, Paper 68-5, p. 37-53.